

UNCLASSIFIED

AD 404 455

*Reproduced
by the*

DEFENSE DOCUMENTATION CENTER

FOR

SCIENTIFIC AND TECHNICAL INFORMATION

CAMERON STATION, ALEXANDRIA, VIRGINIA



UNCLASSIFIED

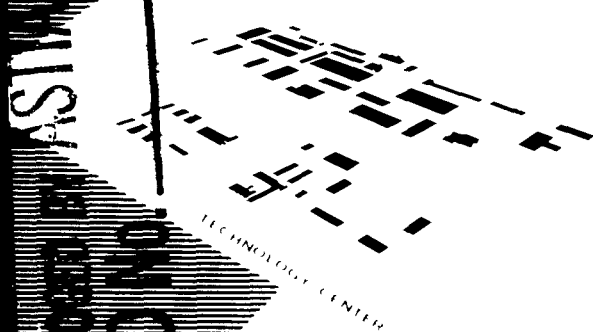
NOTICE: When government or other drawings, specifications or other data are used for any purpose other than in connection with a definitely related government procurement operation, the U. S. Government thereby incurs no responsibility, nor any obligation whatsoever; and the fact that the Government may have formulated, furnished, or in any way supplied the said drawings, specifications, or other data is not to be regarded by implication or otherwise as in any manner licensing the holder or any other person or corporation, or conveying any rights or permission to manufacture, use or sell any patented invention that may in any way be related thereto.

404 455

63-3-4 Copy No. 1

ARF

ARMOUR RESEARCH FOUNDATION OF ILLINOIS INSTITUTE OF TECHNOLOGY



ARMOUR RESEARCH FOUNDATION

TECHNOLOGY CENTER

MAY 20 1963
RECEIVED
S.A.A.

NOTE: Effective June 1, 1963, the name of Armour Research Foundation of Illinois Institute of Technology will change to IIT RESEARCH INSTITUTE.

EVALUATION AND IMPROVEMENT OF RADAR
BEACON SYSTEMS

Report Nr. 2
Contract Nr. DA 36-039 SC-90693
DA Project Nr. 3C16-19-001
ARF Project Nr. E179
Second Quarterly Progress Report
1 September 1962 - 30 November 1962

U. S. Army Electronics Res. and Dev. Lab.
Fort Monmouth, New Jersey

EVALUATION AND IMPROVEMENT OF RADAR

BEACON SYSTEMS

Report Nr. 2

Contract Nr. DA 36-039 SC-90693
ARF Project Nr. E179

SMSA-RD-EID-013, 19 January 1962

DA Project Nr. 3C16-19-001

Second Quarterly Progress Report
1 September 1962 - 30 November 1962

The object of this study program is to establish system parameters and technical specifications for a coherent beacon and to determine the feasibility of using tunnel diodes, varactor diodes, and other solid state devices to advance the art of radar beaconry.

Prepared by

J. Feldman
S. Kazel
R. Standley
P. Toulis

of

ARMOUR RESEARCH FOUNDATION
of Illinois Institute of Technology
Technology Center
Chicago 16, Illinois

for

U. S. Army Electronics Res. and Dev. Lab.
Fort Monmouth, New Jersey

TABLE OF CONTENTS

	<u>PAGE</u>
PURPOSE	iii
ABSTRACT	iv
CONFERENCES	v
I. INTRODUCTION	1
II. TECHNICAL DISCUSSION	1
A. Tunnel Diode Amplifiers - Theory and Practice	1
B. Impedance Matching and Synthesis Techniques for Tunnel Diode Amplifier Circuits	12
C. Design of a C-Band Tunnel Diode Amplifier	19
D. Experimental Results	31
E. Low Level Detection By Tunnel Diodes	43
F. A Proposed Three Frequency Source Using Harmonic Generation Techniques	45
G. Electronically Tunable Tunnel Diode Oscillator	48
H. 1. Doppler Tracking Errors Due to Frequency Instability of the Tracking Loop Voltage Controlled Oscillator	48
2. Tracking Loop	49
III. CONCLUSIONS	57
IV. PROGRAM FOR NEXT INTERVAL	58
V. IDENTIFICATION OF PERSONNEL	59
APPENDIX A	
APPENDIX B	
APPENDIX C	
REFERENCES	

LIST OF ILLUSTRATIONS

<u>FIGURE</u>		<u>PAGE</u>
1	TRANSMISSION TYPE AMPLIFIER	2
2	REFLECTION TYPE AMPLIFIER	2
3	RESISTANCE OF A CIRCULATOR VS FREQUENCY	6
4	REACTANCE OF A CIRCULATOR VS FREQUENCY	7
5	SCHEMATIC FOR STABILITY ANALYSIS	8
6	HYBRID AMPLIFIER	8
7	TYPICAL SECTION OF CASCADED DIODE AMPLIFIER	11
8	LOADS APPLICABLE TO GREEN'S PROCEDURE	11
9	SCHEMATIC FOR GAIN RIPPLE ANALYSIS	16
10	WEINBERG'S NETWORK	16
11	CIRCULATOR - COUPLED TUNNEL DIODE AMPLIFIER	21
12	SERIES AND PARALLEL EQUIVALENT CIRCUITS OF TUNNEL DIODE	21
13	DIAGRAM OF A CIRCULATOR - COUPLED TUNNEL DIODE AMPLIFIER	23
14	MAXIMUM NOISE FIGURE OF A TUNNEL DIODE (D4168D) AMPLIFIER VS FREQUENCY	28
15	TUNNEL DIODE AMPLIFIER WITH FEEDBACK CORRESPONDING TO FIG. 13	23
16	CROSS-SECTIONAL VIEW OF A RIDGED-WAVEGUIDE C-BAND TUNNEL DIODE AMPLIFIER	32
17	DIAGRAM OF A 5.65 KMC TUNNEL DIODE AMPLIFIER	33
18	GAIN VERSUS FREQUENCY DIAGRAM OF TUNNEL DIODE AMPLIFIER	34
19	GAIN VERSUS INPUT POWER DIAGRAM OF TUNNEL DIODE AMPLIFIER	36

LIST OF ILLUSTRATIONS Con't

<u>FIGURE</u>		<u>PAGE</u>
20	DIAGRAM ILLUSTRATING RELATIVE OUTPUT POWER VERSUS INPUT POWER OF TUNNEL DIODE AMPLIFIER	37
21	DIAGRAM ILLUSTRATING RELATIVE OUTPUT POWER VERSUS INPUT POWER OF TUNNEL DIODE AMPLIFIER	38
22	D. C. BIASING CIRCUIT OF TUNNEL DIODE AMPLIFIER	39
23	D. C. BIASING CIRCUIT OF TUNNEL DIODE AMPLIFIER INCLUDING LEAD INDUCTANCE	39
24	EQUIVALENT D. C. BIASING CIRCUIT	42
25	MODIFIED D. C. BIASING CIRCUIT AT LOW FREQUENCIES	42
26	TRI-BAND HARMONIC GENERATION SOURCE	46
27	SCHEMATIC OF VARACTOR TUNABLE TUNNEL DIODE OSCILLATOR	48
28a	BLOCK DIAGRAM	51
28b	REVISED BLOCK DIAGRAM	51

EVALUATION AND IMPROVEMENT OF
RADAR BEACON SYSTEMS

PURPOSE

The program is concerned with two diverse areas relating to radar-beacon systems: 1) solid state microwave component design and evaluation and 2) coherent radar beacon system analysis. Included as a part of the first area is the establishment of design criteria for those solid state devices which could be used advantageously in radar-beacon systems. The analysis of the coherent beacon has been undertaken to permit quantitative evaluation of achievable system performance and to establish a basis for performance specification for future equipment developments.

EVALUATION AND IMPROVEMENT OF
RADAR BEACON SYSTEMS

ABSTRACT

The results of a partial literature survey on tunnel diode amplifiers are presented. The gap existing between the analytical work and practical design is discussed. Limitations of presently available synthesis techniques are pointed out along with the practical problems which these limitations impose. Results on an experimental C-band amplifier are presented. Sensitivity data on a commercial available backward diode is also presented. The anticipated performance of a proposed high power harmonic generation system is discussed. Preliminary analysis of a varactor tunable tunnel diode oscillator is presented. Results of additional theoretical work on the coherent Doppler radar are briefly discussed.

CONFERENCES

Date: 6 and 7 November 1962

Place: White Sands Missile Range

Personnel:

D. Samuelson	WSMR
R. Cathey	WSMR
D. Wise	WSMR
S. Kazel	ARF
J. Ludwig	ARF
R. Standley	ARF

Progress in the areas of tunnel diode devices and the coherent beacon was reviewed. Future work and expected results were discussed. The possibility of deriving coherent beacon specification from the analytical work was also discussed.

FACTUAL DATA

EVALUATION AND IMPROVEMENT OF RADAR BEACON SYSTEMS

I. INTRODUCTION

The work on this program is concentrated in two rather diverse areas relating to radar beacon systems. The first area is concerned with the determination of design techniques for solid state devices applicable to a radar beacon system. Section II A contains information obtained from several references on the synthesis and design problem associated with tunnel diode amplifiers. In Section II B and II C, experimental results on a C-band amplifier design and a backward diode detector are presented.

II. TECHNICAL DISCUSSION

A. Tunnel Diode Amplifiers - Theory and Practice

1. Introduction

A number of excellent reports have appeared in the literature which survey tunnel diode amplifier theory.^{1, 2, 3} In this section of the report portions of the more important theoretical work is summarized and commented on regarding their use in practical designs. Particular attention is given to the restrictive assumptions used in developing the theory. The theory will not be presented in detail. For the most part results will be cited which when properly used will serve as a means for predicting the performance of the various design configurations.

2. Single Diode Amplifiers^{1, 2, 4}

(a). Transmission Type

A series type of transmission amplifiers is shown in Figure 1. The transducer gain for this type of amplifier is readily shown to be

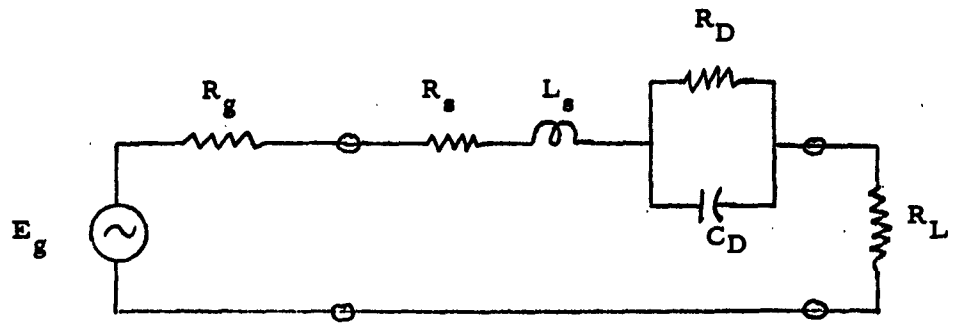


FIG. 1 TRANSMISSION TYPE AMPLIFIER

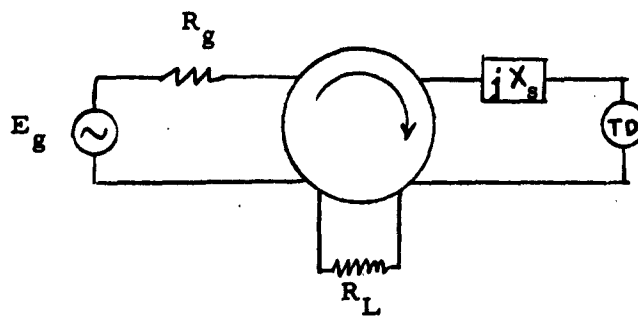


FIG. 2 REFLECTION TYPE AMPLIFIER

$$G = \frac{4R_g R_L}{\left[(R_L + R_s + R_g) - |R'_D| \right]^2} \quad (1)$$

under tuned conditions, i. e. the total loop reactance is zero. In equation (1)

R'_D is the series equivalent tunnel diode resistance,

$$R'_D = \frac{R_D}{1 + \omega^2 C_D^2 R_D^2} \quad (2)$$

Let $\alpha = \frac{|R'_D|}{R_T}$ where $R_T = R_g + R_L + R_s$

$$G = \frac{4R_g R_L}{R_T^2} \left[\frac{1}{1 - \alpha} \right]^2 \quad (3)$$

The percentage change in G with respect to the percentage change in α gives a measure of circuit stability. This can be shown to be

$$S = \frac{2\alpha}{1 - \alpha} \quad (4)$$

For stability α must be less than + 1. For high gain α must approach 1 so that high gains impose serious stability problems. It can also be shown that

$$R_g = R_s + R_L$$

is required for maximum gain for a given

In the practical case R_g and R_L represent antenna and load impedances respectively. In view of this fact maintaining $\alpha < 1$ over a very broadband imposes serious stability problems. For this reason little use of this type of amplifier has been made at microwave frequencies. Section C below

ARMOUR RESEARCH FOUNDATION OF ILLINOIS INSTITUTE OF TECHNOLOGY

indicates the severity of the impedance variation problem.

(b). Reflection Type Amplifier with Circulators ^{1, 2, 4}

At microwave frequencies circulators are employed to ease the stability problem. A circulator type of amplifier is shown in Figure 2. The reactance jX represents a tuning reactance. The gain of the amplifier is given by

$$G = |\Gamma|^2 = \left| \frac{(R_s + R'_D) - R_L}{(R_s + R'_D) + R_L} \right|^2 \quad (5)$$

where Γ is the input reflection coefficient. Tuned conditions have been assumed. Letting

$$\alpha = \frac{(R_s + R'_D)}{R_L} \quad ,$$

$$G = \left| \frac{1 + \alpha}{1 - \alpha} \right|^2 \quad (6)$$

the amplifier bandwidth is

$$\Delta \omega = \frac{1}{|r_L| C_D} \left(\frac{1 - \alpha}{\alpha} \right) \left(1 - \frac{R_s}{|R'_D|} \right) \quad (7)$$

The exact noise figure is

$$F = 1 + \frac{T}{T_o} \left\{ \frac{G_{eq} R'_D + R_s}{G_D R_L} \right\} \quad (8)$$

where

T_o = source temperature (°K)

$$G_{eq} = \frac{eI_o}{2kT}$$

T = diode temperature (°K)

k = Boltzmann's Constant

$I_o = \text{dc bias current}$

If $T = T_o$, F may be put in the form,

$$F = \frac{1 + \frac{G_{eq}}{G_D}}{\left(1 - \frac{R_s}{|R_D|}\right) \left(1 - \frac{\omega^2}{\omega_{co}^2}\right)} \quad (9)$$

where $\omega_{co} = \text{resistive cutoff frequency of the diode. Eq. (9) assumes}$

$$\frac{R_s}{|R_D|} \ll 1,$$

$$(1 - \frac{\omega^2}{\omega_{co}^2}) < 0.5 .$$

Similar results may be derived for the shunt tuned amplifier.

In the majority of the theoretical developments ideal circulator characteristics are assumed. However in the practical case the input impedance of a matched circulator is far from constant (See Figure 3 and 4).

(c). Stability Requirements

Each of the amplifiers thus far described may be considered to have the form shown in Figure 5. A transient analysis of this circuit yields the following inequalities which must be satisfied for stability.

$$|R_D| > R_T > \frac{L_T}{|R_D| C_D} \quad (10)$$

Equation 10 must be satisfied at all frequencies. This requires that complete knowledge of the circuit impedances be obtained at all frequencies. In the practical case, the general functional forms of R_D , R_T , and L_T must be determined by experimental methods. It is this difficulty which prevents general design criteria from being established.

ARMOUR RESEARCH FOUNDATION OF ILLINOIS INSTITUTE OF TECHNOLOGY

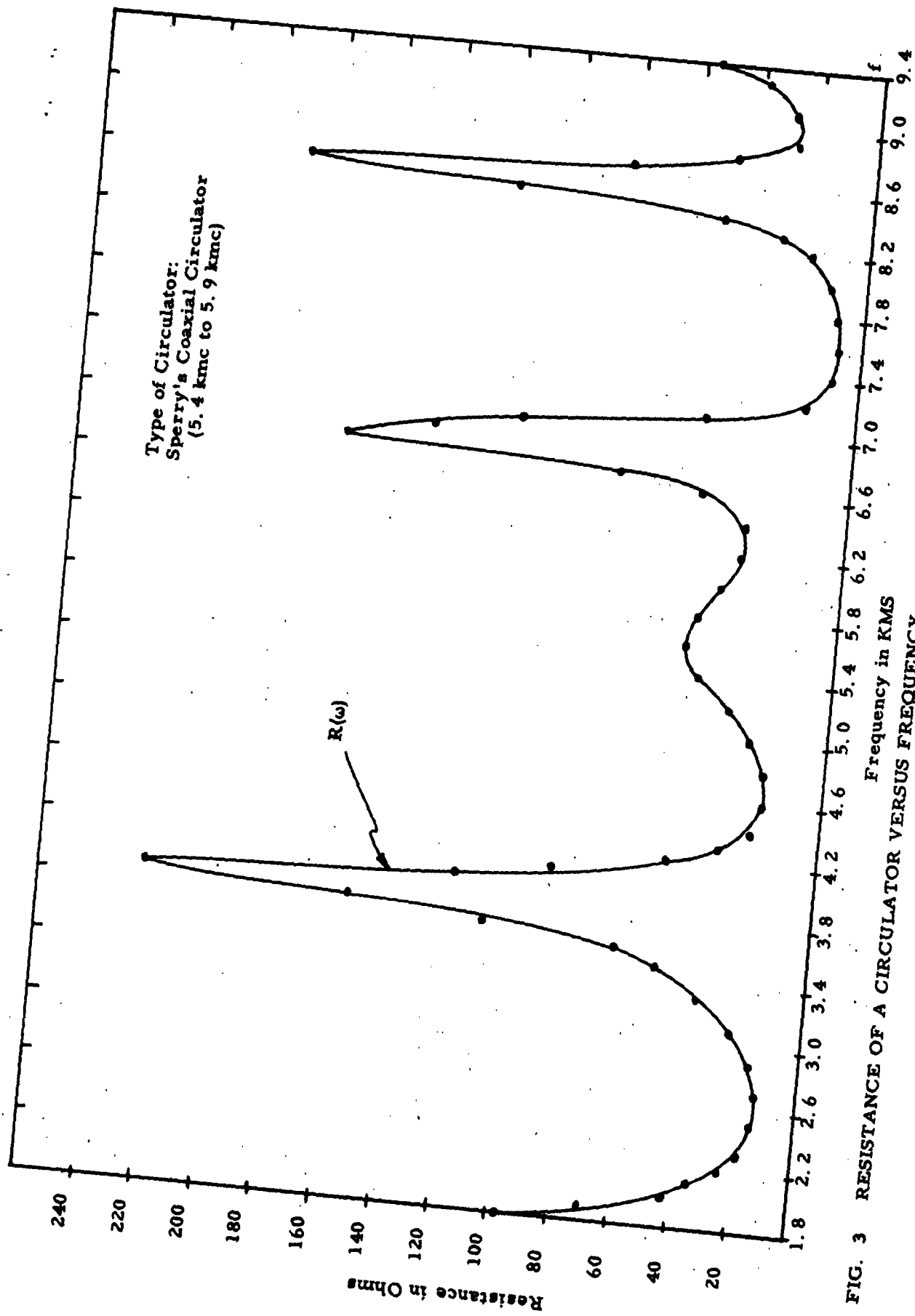


FIG. 3 RESISTANCE OF A CIRCULATOR VERSUS FREQUENCY

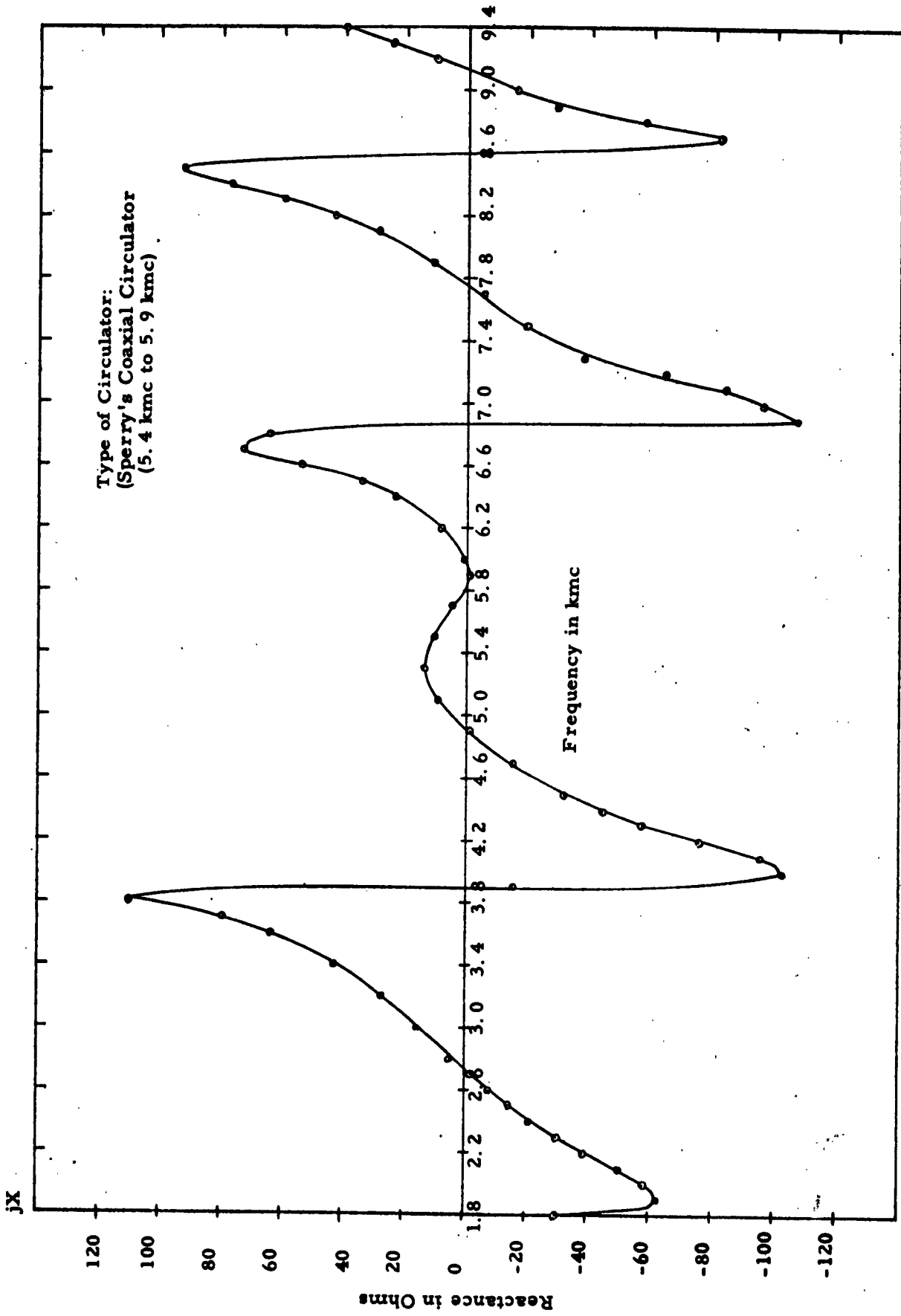


FIG. 4 REACTANCE OF A CIRCULATOR VERSUS FREQUENCY

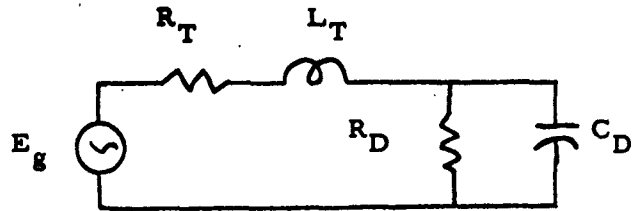


FIG. 5 SCHEMATIC FOR STABILITY ANALYSIS

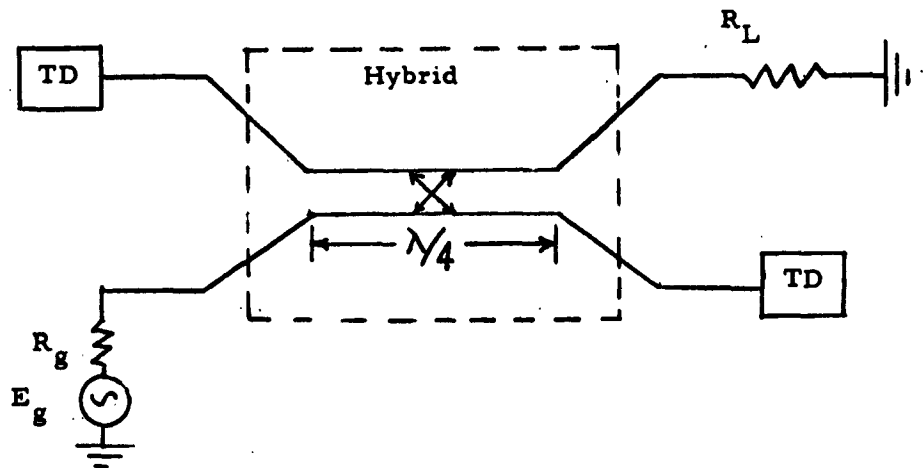


FIG. 6 HYBRID AMPLIFIER

It should also be mentioned that stability in the d. c. biasing circuit is one of the foremost problems in the design of practical amplifiers. Stray lead inductances and high source impedance severely effect the biasing problem. For this reason it is often necessary to use mercury cells as the d. c. source. In addition pyrofilm resistors are usually required to avoid the lead inductance of the familiar carbon type resistor. For a discussion of d. c. biasing circuits see Section IIC4.

3. Hybrid Two-Diode Amplifier²

In the hybrid coupled amplifier isolation is achieved by using a balanced transmission line coupler as shown in Figure 6. This type of device has been thoroughly analyzed for the familiar quarter-wave three db coupler.¹ The transducer gain is

$$G = |G_V|^2 \left[\frac{2k \sqrt{1 - k^2} \sin \theta}{1 - k^2 \cos^2 \theta} \right]^2 \quad (11)$$

where

$$\begin{aligned} |G_V|^2 &= \frac{(1 + jX)^2 + (B/Y_0)^2}{(1 - jX)^2 + (B/Y_0)^2} \\ &= \frac{|G|}{Y_0} \end{aligned} \quad (12)$$

Y_0 = hybrid characteristic impedance

$|G|$ = diode conductance

B = diode susceptance

k = hybrid coupling factor .

Since the transmission line hybrids are inherently broadband, attempts should be made to match the diode impedance to the coupler over as broad a

band as possible. Impedance matching filters may be used for this purpose. The literature contains a fairly comprehensive discussion on this technique. Optimum matching from a theoretical point of view is discussed below.

4. Cascading Techniques

An analysis has been presented of an idealized one-dimensional model of a transmission line periodically shunt loaded by tunnel diodes.¹ Floquet's theorem was applied in the infinite line case so that

$$\begin{bmatrix} V_n \\ I_n \end{bmatrix} = \begin{bmatrix} V_0 \\ I_0 \end{bmatrix} e^{-\gamma n l} \quad (13)$$

where $\gamma = \alpha + j\beta$ = propagation constant of the loaded line
 l = length of transmission line between diodes.

Figure 7 shows a typical section.

The results of the analysis were a set of determinantal equations for α and β :

$$\cosh \alpha l \cos \beta l = \cosh \alpha_0 l \cos \beta_0 l + G \sinh \alpha_0 l \cos \beta_0 l + B' \cosh \alpha_0 l \sin \beta_0 l \quad (14)$$

$$\sinh \alpha l \sin \beta l = -\sinh \alpha_0 l \sin \beta_0 l + B' \sinh \alpha_0 l \cos \beta_0 l - G \cosh \alpha_0 l \sin \beta_0 l \quad (15)$$

where α_0, β_0 refer to the propagation constant of the unloaded line, and $G + jB'$ is the equivalent diode admittance. The above equations when properly interpreted yield the limits on α and β as well as defining the frequency ranges in which gain is obtained.

The more practical case of the finite line was also analyzed. The amplifier gain was shown to be

$$G_{db} = 8.686 \log_{10} |N| \quad (16)$$

(where N = total number of diodes)

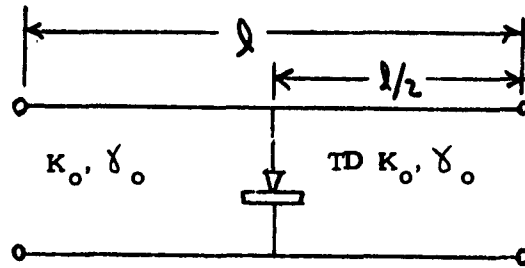


FIG. 7 TYPICAL SECTION OF CASCADED DIODE AMPLIFIER

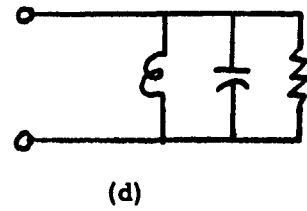
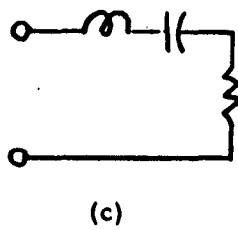
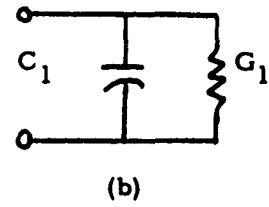
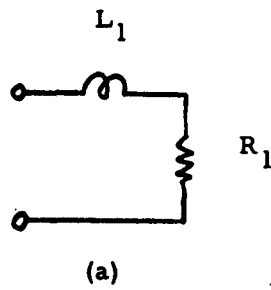


FIG. 8 LOADS APPLICABLE TO GREEN'S PROCEDURE

for the condition that the circuit be terminated in an impedance

$$Z_o = \sqrt{\frac{K_o^2}{y^2 K_o^2 + 1 + 2y K_o \coth \gamma L}} \quad (17)$$

where $y = \frac{G + jB'}{2}$

K_o = characteristic impedance of connecting transmission line.

No effort was made to determine the performance of such an amplifier using typical diodes. Neither was the effects of K_o , y , γ_o on bandwidth determined. One serious practical restriction on amplifiers of this type is that identical tunnel diodes do not exist so that y will in general differ for each diode. Note that this problem was also one of the serious difficulties with traveling wave parametric amplifiers using varactor diodes.

5. Broadband Tunnel Diode Amplifier Theory

Smilen has presented a theory for optimum single diode amplifiers in both transmission and reflection form.⁵ The "optimum design" is obtained by use of properly designed equalizer circuits. The reader should be referred to reference 5 for the details of the procedure. In order to simplify the analysis, the series inductance in the diode equivalent circuit was neglected. This limits the frequency range over which the analysis holds to well below the diode self-resonant frequency. Therefore, the procedure can not be well adapted to microwave applications.

B. Impedance Matching and Synthesis Techniques for Tunnel Diode Amplifiers Circuits

1. Introduction

The literature contains several references to impedance matching of

negative resistance devices.^{6, 9} This portion of the report reviews the major contributions and discusses the problems involved in applying such techniques at microwave frequencies. Included is an outline of Green's approach to matching a low pass prototype load consisting of a frequency invariant positive resistor plus an inductor or capacitor¹⁰. The application of impedance matching filter networks as applied to varactor diodes is also reviewed. The applicability of Weinberg's synthesis procedures at microwave frequencies is evaluated from a practical point of view.

2. Impedance Matching Filters

Matthaei was the first to recognize that filter networks might be useful as a means of increasing the bandwidth of parametric amplifiers. The basic approach was to use filter networks which presented the optimum impedance to the varactor diode over as broad a frequency range as possible. By making the stray reactances of the diode package a part of the first resonator of the matching network, the bandwidth restrictions imposed by C_0 , the fixed parasitic capacitance, were relaxed. In Matthaei's first paper the prototype elements of conventional Tchebysheff filters were used.⁷ The gain versus frequency plot was then obtained by means of a computer. Trial and error adjustments to the prototype were then made to obtain the nearly optimum filter design. In a latter publication Green's work was mentioned by Matthaei in connection with the optimum impedance matching network.⁶ Green's design equations were adapted to a convenient form for calculation of the prototype elements in terms of the conventional parameters used in present day microwave filter design.

Several authors have presented the results of amplifiers designed using Matthaei's analysis. In practice the major difficulties encountered are:

- 1) Lack of knowledge of the equivalent circuit parameters for a given diode.
- 2) The matching network derived is in the form of a lumped element prototype. The microwave network corresponding to the prototype is not unique.

The first difficulty may be overcome by experimentally adjusting the first resonator of the filter to give the proper slope parameter. The second difficulty usually proves to be the most serious. The form of the microwave network should be selected to yield a design which is easy to construct. Trial and error methods are required to determine the most suitable form. Additional requirements on the selected network are that it not have spurious pass bands at or near the pump and idler frequencies and that biasing of the diode can be easily achieved. The latter requirements are difficult to achieve above about 2 kmc for present day diodes.

The above techniques were used by the author in the design of an electronically tunable filter at C-band. Spurious resonances and isolation of the biasing network prevented completion of the design in the time allotted to the project.

3. Green's Synthesis Procedure for Optimum Matching Networks

The matching problem analyzed by Green is the following. Design a non-dissipative Tchebysheff coupling network such that when terminated in Z , the magnitude of the input reflection coefficient is less than or equal to some \max at all frequencies within a specified band. Z is to be restricted to the simplified case consisting of a single reactive element combined with a resistor. By proper frequency transformation, R, L, C band pass combination is also allowed. The four types of Z thus considered are shown in Figure 8.

In terms of the network parameters the problem may be restated as follows.

Given the load decrement, defined by

$$D_1 = \frac{R_1}{\omega\beta L_1} \quad \text{for the series case} \quad (18)$$

$$D_1 = \frac{G_1}{\omega\beta C_1} \quad \text{for the parallel case} \quad (19)$$

and the desired bandwidth $\omega\beta$ along with number of branches to be used, find the value of $\frac{D_n}{D_1}$ which makes $|\Gamma|_{\max}$ minimum within the band. (D_n is the input decrement parameter). Green solved this problem, and the results are presented in the form of design curves from which the matching network circuit elements can be obtained once D_1 , $\omega\beta$ and the minimum value of $|\Gamma|_{\max}$ have been prescribed.

The applicability of this design procedure to the problem of matching loads consisting of a single reactive element in combination with a negative resistance will now be discussed. It can be shown that for such a load the gain response will contain ripples much larger in magnitude than the corresponding ripples when the resistance is positive.¹¹ Consider the network of

Figure 9. If R_o is positive then

$$\Gamma_1 = \frac{Z_1 - R_o}{Z_1 + R_o} \quad (20)$$

$$\Gamma_2 = \frac{Z_2 - R_2}{Z_2 + R_2} \quad (21)$$

$$|\Gamma_1| = |\Gamma_2| \quad (22)$$

Since $|\Gamma_2|^2$ is the transducer gain so is $|\Gamma_1|^2$. Suppose the matching

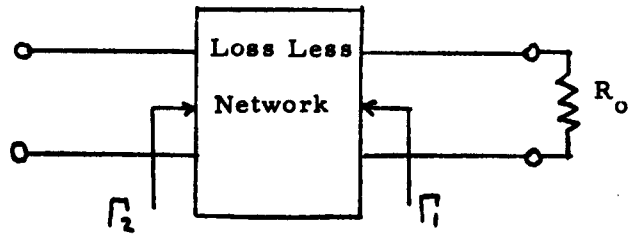


FIG. 9 SCHEMATIC FOR GAIN RIPPLE ANALYSIS

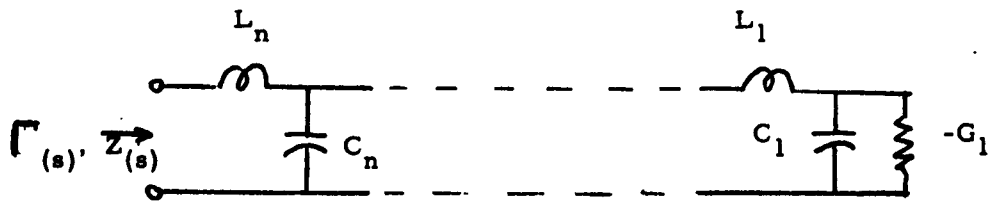


FIG. 10 WEINBERG'S NETWORK

network has to be designed by Green's procedure. Now let $R_o = -R_o'$, i. e. consider the terminating resistance as being negative. Then

$$\left| \Gamma_1' \right| = \left| \frac{Z_1 + R_o'}{Z_1 - R_o'} \right| = \frac{1}{\left| \Gamma_1 \right|} \quad (23)$$

Therefore, the ripples in $\left| \Gamma_1' \right|$ will be larger than those in $\left| \Gamma_1 \right|$. Knowing $\left| \Gamma_1 \right|$, however, $\left| \Gamma_1' \right|$ can be easily determined. It is also possible to work backwards so that if the allowable ripple in $\left| \Gamma_1' \right|$ is prescribed, the allowable ripple in Green's network can be calculated. The method for accomplishing this will not be presented here because of the triviality of the development.

The question of primary importance in attempting to apply Green's procedure to tunnel diode amplifiers is, can the diode be represented as a negative resistor combined with a single reactive element. The answer is no, in general. As mentioned below regarding Weinberg's procedure, R_s and L_s are considerably important at microwave frequencies.

4. Weinberg's Synthesis Procedure.

Weinberg considered the matching problem depicted in Figure 10 for the reflection type tunnel diode amplifier. A synthesis procedure was derived for realizing a reflection coefficient having either a Butterworth or Tchebysheff frequency variation. The procedure is outlined below for the Butterworth response. In terms of the complex frequency variable S ,

$$\Gamma(s) \Gamma(-s) = \frac{K - S^{2n}}{1 - S^{2n}} \quad (24)$$

The network input impedance may be put in the forms (for n odd)

$$Z(s) = \frac{1 + \Gamma(s)}{1 - \Gamma(s)} \quad (25)$$

$$\frac{\sum_{k=0}^{n-1} a_k S^k}{\sum_{k=0}^{n-1} b_k S^k} \quad (26)$$

$$= \frac{-\frac{Z_{11}}{G_1} + |Z|}{Z_{22} - \frac{1}{G_1}} \quad (27)$$

By proper manipulation of equation 26 and comparing to equation 27 it can be shown that

$$Z_{22} = \frac{\frac{a_0}{b_0} (b_{n-1} S^{n-1} + b_{n-3} S^{n-3} + \dots + b_1)}{b_n S^n + b_{n-2} S^{n-2} + \dots + b_1 S} \quad (28)$$

Similar results may be derived for n even in terms of y_{22} . For a given n , the right half plane zeros and left half plane poles of equation 24 are found.

$\Gamma(s)$ may then be formed. This $\Gamma(s)$ when used in equation 25 gives the corresponding $Z(s)$. $Z(s)$ is then manipulated to make $Z_{22}(s)$ recognizable. Knowing $Z_{22}(s)$ the desired network may then be developed in the form of a Cauer ladder.

It should be recognized that the above analysis applies to the low pass prototype of the desired network. Well known frequency transformations are employed to yield the band pass form of the network. One additional fact of considerable importance is that the above procedure was derived so that the first element of the matching network nearest $-G_1$ would be a shunt capacitance. Then by proper frequency scaling the shunt capacitance may be made to equal the shunt capacitance of the diode equivalent circuit. Let ω_n be the scaling frequency and ω_c be the frequency at which the power out is one-half the maximum. In terms of these parameters it can be shown that the normalized bandwidth of the resulting network is

$$\frac{\omega_c C_1'}{G_1'} = \frac{2 \sin \pi/2n}{\left(1 - \frac{2}{K}\right)^{1/2n} (K^{1/2n} - 1)} \quad (29)$$

For the analysis, Weinberg assumed a diode equivalent circuit consisting of a frequency invariant resistance shunted by a capacitance. At microwave frequencies this circuit is not even approximately equivalent to the diode over any appreciable bandwidth. The parasitic inductance and spreading resistance, which have been neglected above, play important roles in practical design work. For this reason Weinberg's synthesis technique gives unrealistic results in the microwave range and therefore must be discarded as an exact design procedure.

C. Design of a C-Band Tunnel Diode Amplifier

1. Basic Considerations

It is well known that a tunnel diode exhibits a negative resistance in its forward biased region. This negative resistance, according to theoretical and experimental results, extends well into the high microwave region. Construction of linear RF amplifiers is possible by using the linear portion of the negative resistance curve. The tunnel diode is particularly suited for broadband applications since it exhibits a negative resistance which is independent of external loading conditions and which varies continuously with frequency. This differs from parametric amplification where the negative resistance, actuated by a CW pump, depends critically on external loading conditions and occurs only in discrete frequency bands.

2. Reflection Type Amplifiers

Transmission type amplifiers will not be considered here for reasons that are discussed in Section IIA 2 of this report.

In utilizing reflection type amplifiers in practical structures, a suitable network is required to separate the incident wave from the amplified reflected wave. There are two possible types of amplifiers that can achieve this separation of waves: the "circulator coupled", and the "hybrid coupled" amplifier. In the former, a three-port or four-port circulator is used to effect the signal separation between input and output waves, Figures 2 and 11. The latter, which is discussed in a previous section, is usually used for wide band applications, where circulators are not available. In this section only the circulator coupled, reflection-type amplifiers will be considered. Results obtained for this amplifier would be directly applicable to hybrid-coupled tunnel diode amplifiers if ideal circulators and hybrids are assumed.

(a). Gain of Circulator-Coupled Amplifiers

In discussing this amplifier, it would be convenient to have the parallel-type equivalent circuit of a tunnel diode. The series and parallel equivalent circuits of a tunnel diode are shown in Figure 12,

where

$$G(\omega) = \frac{|R_{TD}(\omega)|}{|Z_{TD}(\omega)|^2} \quad \text{or} \quad R(\omega) = \frac{|Z_{TD}(\omega)|^2}{|R_{TD}(\omega)|} \quad (30)$$

$$C_D(\omega) = \frac{-X_{TD}(\omega)}{\omega |Z_{TD}(\omega)|^2} \quad (31)$$

$$R_{TD}(\omega) = R_s - \frac{r}{1 + (\omega cr)^2} \quad (32)$$

$$X_{TD}(\omega) = \omega \left[L_s - \frac{cr^2}{1 + (\omega cr)^2} \right] \quad (33)$$

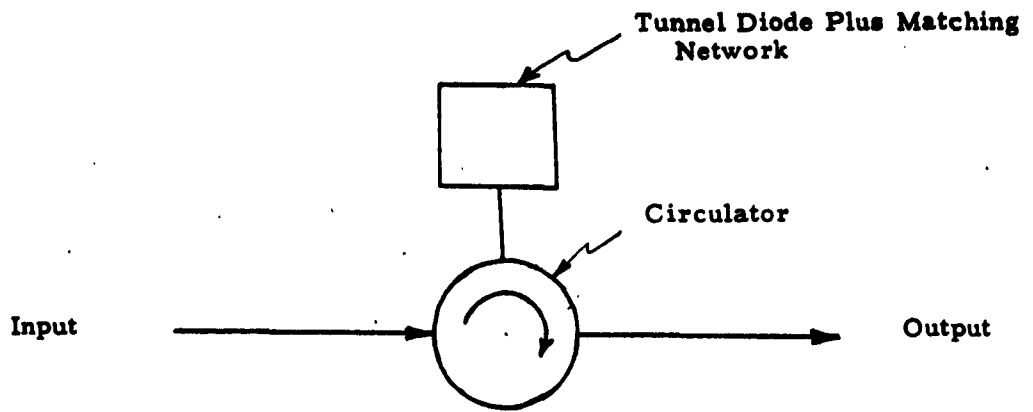


FIG. 11 CIRCULATOR - COUPLED TUNNEL DIODE AMPLIFIER

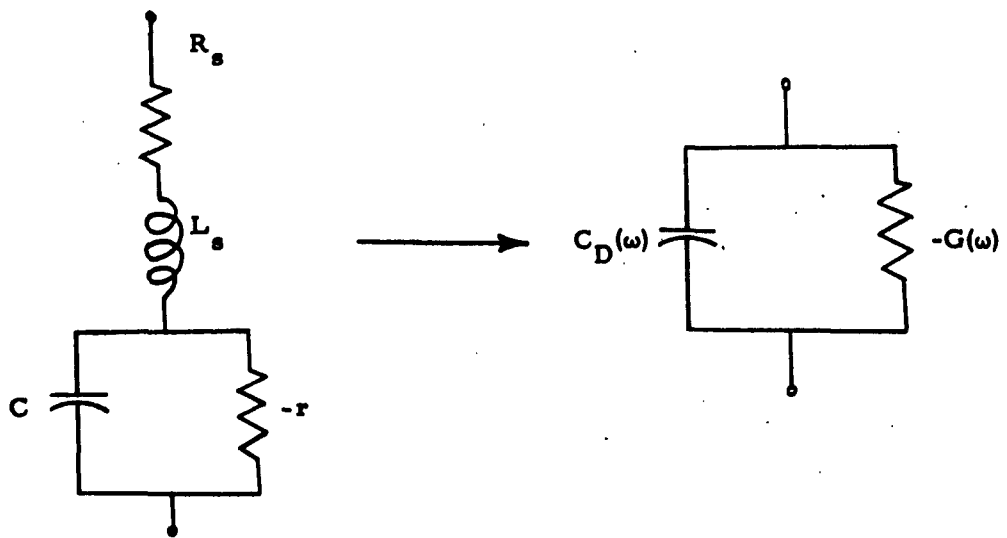


FIG. 12 SERIES AND PARALLEL EQUIVALENT CIRCUITS OF TUNNEL DIODE

$$Z_{TD}(\omega) = R_{TD}(\omega) + j X_{TD}(\omega) \quad (34)$$

The particular amplifier circuit to be considered in this case is that shown in Figure 13. The parallel susceptance $jB(\omega)$ which includes diode parasitics, is used for tuning purposes. The reason for choosing parallel tuning rather than series is because this amplifier is intended to be designed in a waveguide configuration and as such series tuning would be difficult to achieve. The purpose of the quarter-wavelength line is to make the proper impedance transformation so that stability of the amplifier can be accomplished; it is a well-known fact that the impedance level of the external circuitry presented to the tunnel diode must be transformed to a lower one for stability purposes. This fact will be obvious when stability criteria for the amplifier are presented below.

From Figure 13,

$$Y_L = -G + jB \quad (35)$$

and the reflection coefficient at port 2 is,

$$G_p = \left| \Gamma_2 \right|^2 = \left| \frac{Y_o - Y_L}{Y_o + Y_o} \right|^2 = \left| \frac{(Y_o + G) - jB}{(Y_o - G) + jB} \right|^2 \quad (36)$$

where

$\left| \Gamma_2 \right|$ = magnitude of reflection coefficient at port (2),

Y_o = transition line admittance,

G_p = power gain at port (2) .

At the operating frequency, $\omega = \omega_o$.

$$jB(\omega_o) = 0 \quad (37)$$

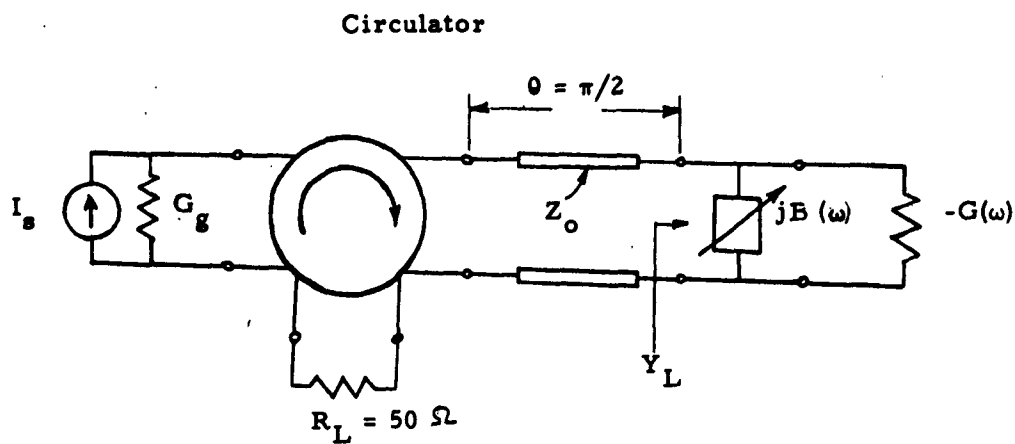


FIG.13 DIAGRAM OF A CIRCULATOR COUPLED TUNNEL DIODE AMPLIFIER

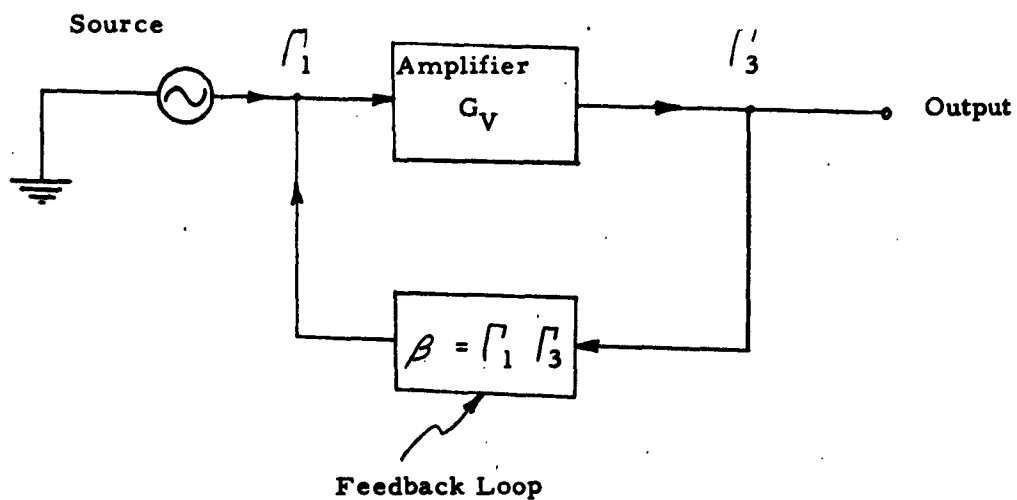


FIG. 15 TUNNEL DIODE AMPLIFIER WITH FEEDBACK CORRESPONDING TO FIG.13.

then Equation (36) becomes,

$$G_p(\omega_s) = \left| \frac{Y_o + G(\omega_s)}{Y_o - G(\omega_s)} \right|^2 \quad (38)$$

By solving Equation (38) for Y_o or Z_o , we have

$$Z_o(\omega_s) = R(\omega_s) \frac{\sqrt{G_p} - 1}{\sqrt{G_p} + 1} \quad (39)$$

Equation (39) indicates the relationship between gain and tunnel diode equivalent resistance at the design frequency. This same equation will be used for the actual design of a C-band tunnel diode amplifier.

For relatively high power gains, say

$$G_p > 100$$

Equation (39) becomes

$$Z_o(\omega_s) = R(\omega_s) \text{ for } G_p > 100. \quad (40)$$

(b). Gain-Bandwidth Product

The gain-bandwidth product of a reflection type tunnel diode amplifier is a function of the rc product of the diode and the coupling network used (jB).

It can be shown that for a single resonator circuit, which is the case here, the following approximate relationship holds: (1, 2)

$$B(\sqrt{G_p} - 1) = \frac{1}{\pi r C} \quad (41)$$

where

B = Bandwidth in cps.

and for high gains, $G_p > 100$, Equation (41) becomes,

ARMOUR RESEARCH FOUNDATION OF ILLINOIS INSTITUTE OF TECHNOLOGY

$$B G_p^{1/2} \doteq \frac{1}{\pi r C} \quad (42)$$

Thus for broadband applications and high gains a tunnel diode must have a small rc product.

As an example, consider Sylvania's D4168D tunnel diode for which,

$$rc = 17.69 \times 10^{-12}$$

and from Equation (42),

$$B G_p^{1/2} = 9.0 \text{ kmc.}$$

Assuming a gain of

$$G_p = 100 \text{ or } 10 \text{ db,}$$

$$B = 900 \text{ mc.} \quad (43)$$

At a frequency of $f_o = 5.65 \text{ kmc}$, percentage-wise the bandwidth is:

$$B = 16\% \text{ at } f_o = 5.65 \text{ kmc.} \quad (44)$$

However, the actual bandwidth of a 5.65 kmc tunnel diode amplifier might be less due to the fact that Equation (42) has been derived under the assumption that the working frequency is to be such that the effect of the series resistance and lead inductance of the tunnel diode may be neglected, which is not actually true in this case.¹² The effect of the transmission line was also neglected. But the result obtained in (44) above indicates that it could be possible to cover the frequency range from 5.4 kmc to 5.9 kmc with a single resonator circuit as the coupling network, since this range is only 8.85% bandwidth at $f_o = 5.65 \text{ kmc}$. Otherwise it would be required to use a more complicated coupling network to achieve broader bandwidths.

(c) Noise Figure of Tunnel Diode Amplifier.

The noise figure of an amplifier can be defined as the ratio of the

total noise at the output to the noise at the output due to an input noise of $k T_o \Delta f$,

$$F = \frac{N_T}{N_o} = 1 + \frac{N_a}{k T_o \Delta f G_p} \quad (45)$$

where

N_a = noise output due to the amplifier network,

T_o = absolute temperature of source in degrees Kelvin,

k = Boltzman constant (1.37×10^{-23} joule per degree),

f = Bandwidth associated with the noise in cycles.

It can be shown that the noise figure of a tunnel diode amplifier for very large gains is given by the following formula:

$$F_{\max} = \frac{1 + K_1}{\left(1 - \frac{R_s}{r}\right) \left(1 - \frac{f^2}{f_{or}^2}\right)} \quad (46)$$

for G_p very large,

where

$K_1 = 20 I_o r$ = noise constant,

$$I_o = \frac{I_p + I_v}{2},$$

f_{or} = tunnel diode resistive cutoff frequency.

For Sylvania's D4168D tunnel diode,

$$-r = -44 \ \Omega$$

$$R_s = 2.6 \ \Omega$$

$$C = 0.4 \text{ pf}$$

$$I_o = 1.82 \text{ ma}$$

and

$$f_{or} = \frac{1}{2\pi r C} \sqrt{\frac{r}{R_s} - 1} = 36 \text{ kmc},$$

$$K_1 = 20I_o r = 1.60$$

then from Equation (46) we get,

$$F_{\max} \left| \begin{array}{l} = 2.84 \text{ or } 4.53 \text{ db} \\ f_o = 5.65 \text{ gc} \end{array} \right. \quad (48)$$

In Figure 14 F_{\max} is plotted as function of frequency for this particular tunnel diode. It can be seen that for the frequency range of interest (5.4 kmc to 5.9 kmc) the maximum noise figure is approximately 4.5 db and almost constant. Again it should be mentioned that this noise figure is for very large gains. Thus, the actual noise figure of the amplifier will be

$$F \leq 4.5 \text{ db}$$

in the frequency range

$$5.4 \text{ kmc} \leq f \leq 5.9 \text{ kmc}.$$

(d). Stability Conditions

Stability in this case is considered from a different point of view, but the restrictions obtained are similar to those discussed in a previous section IIA2c of this report.

The following definitions refer to Figure 15.

Let

K = Voltage gain with feedback,

G_v = Voltage gain without feedback,

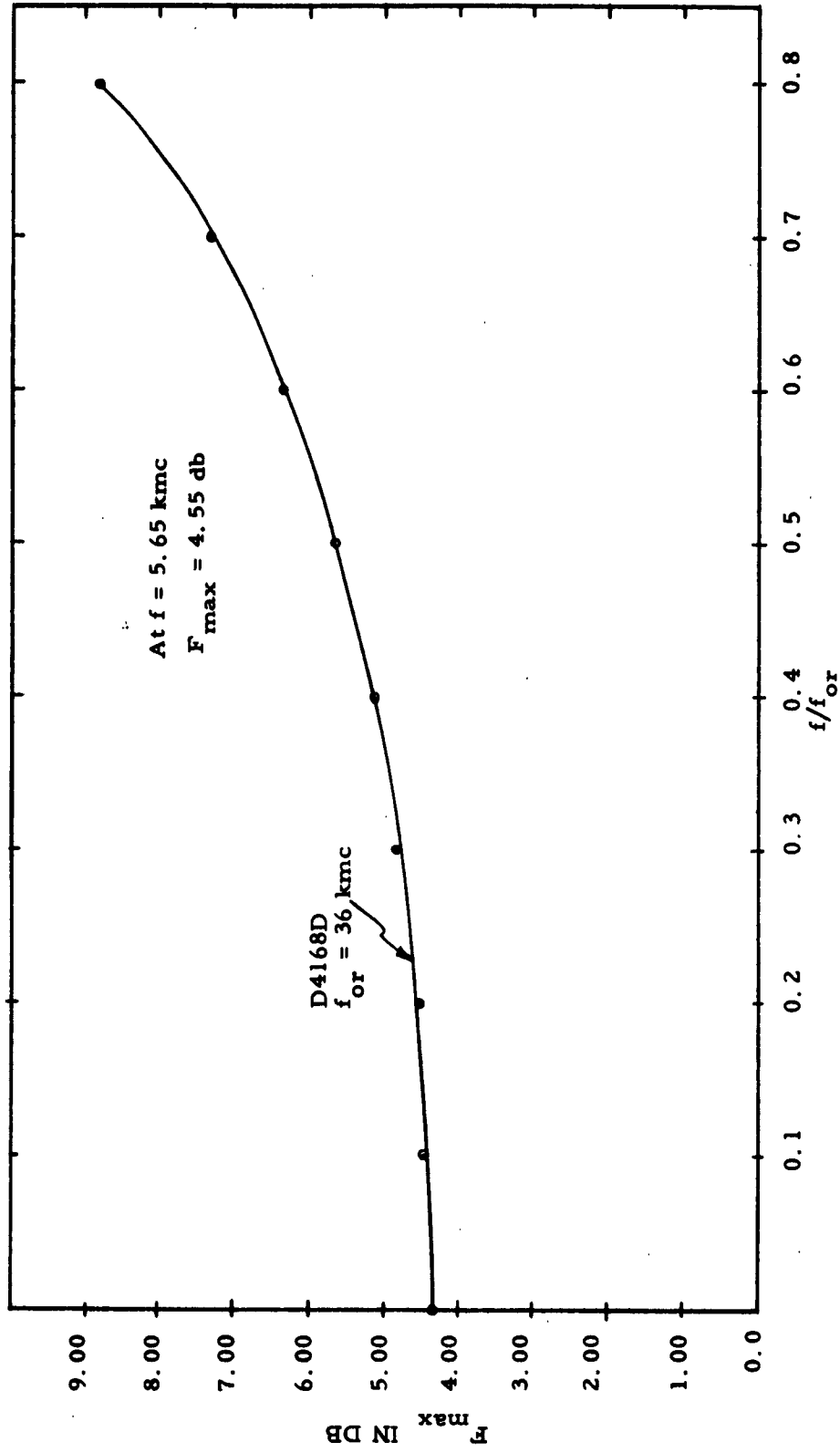


FIG. 14. MAXIMUM NOISE FIGURE OF A TUNNEL DIODE (D4168D) AMPLIFIER VS FREQUENCY

$|\beta|$ = Voltage gain of feedback loop.

Then

$$K = \frac{G_v}{1 - \beta G_v} \quad (49)$$

and for the amplifier to be stable

$$|\beta| G_v < 1$$

or

$$|\Gamma_1| |\Gamma_3| G_v < 1$$

or

$$G_p |\Gamma_1|^2 |\Gamma_3|^2 < 1. \quad (50)$$

This relationship shows that the reflections at ports (1) and (3) must be low enough for a certain gain if the amplifier is to be stable.

Considering an example, let

$$|\Gamma_1| = |\Gamma_3| = \frac{\text{VSWR} - 1}{\text{VSWR} + 1}$$

and for Sperry's 5.4 kmc to 5.9 kmc coaxial circulator

$$\text{VSWR}_{\text{max}} = 1.25$$

then inequality (50) becomes,

$$G_p < 38 \text{ db} \quad (51)$$

which means that if a tunnel diode amplifier is to be stable, its gain should not be greater than 38 db.

In the following sections, restriction (51) and eqa. (39) will be used in designing a C-band, circulator coupled tunnel diode amplifier.

3. Design of a 5.65 kmc Reflection - Type, Circulator - Coupled Tunnel Diode Amplifier.

For Micro State's MS1102 tunnel diode the circuit parameters are:

$$r = 35 \Omega \text{ (minimum)}$$

$$C = 0.6 \text{ pf}$$

$$R_s = 4.0 \Omega$$

$$L_s = 0.3 \text{ nph}$$

This amplifier is to have a power gain of $G_p = 20 \text{ db} < 38 \text{ db}$ at $f_o = 5.65 \text{ kmc}$.

Referring now to Figure 12, the circuit parameters of the parallel equivalent circuit of this diode are:

$$R(\omega_o) = \left| \frac{Z_{TD}(\omega_o)}{R_{TD}(\omega_o)} \right|^2 = 20.55 \Omega \quad (52)$$

$$C_D(\omega_o) = - \frac{X_{TD}(\omega_o)}{\omega_o |Z_{TD}(\omega_o)|^2} = 0.455 \text{ pf} \quad (53)$$

and for a gain of

$$G_p = 20 \text{ db}$$

Equation (10) becomes,

$$Z_o(\omega_o) = R(\omega_o) \frac{\sqrt{G_p} - 1}{\sqrt{G_p} + 1} = 20 \Omega \quad (54)$$

Since $G_p = 20 \text{ db}$, the amplifier will be stable according to inequality (51).

The characteristic impedance of the quarter wavelength transformer (see Figure 13) being low (25Ω), it was decided to use ridged-waveguide circuitry. The reasons for choosing this type of circuit configuration is the fact that ridged-waveguides exhibit broadband characteristics and that if design criteria for a C-band tunnel diode amplifier can be established it would be relatively easy to extend the design of such amplifiers at higher frequencies.

Design formulas and graphs on ridged-waveguides can be found in reference (13). For methods of coupling a 50Ω coaxial line to a ridged-waveguide refer to reference (14). Using these two references, it is a straight-forward problem to design the tunnel diode amplifier shown in Figure 13; thus, a detailed design procedure will not be given here.

Figure 16 shows the diagram of an actual amplifier that is designed in a ridged-waveguide configuration. In this figure, the movable short on the left hand side is used to tune out the diode susceptance at the working frequency, whereas the one on the right hand side is to provide a better matching between the 50Ω coaxial line and the 20Ω quarter-wavelength transformer. At the beginning it was necessary to build the amplifier with two coaxial inputs similar to the one shown in the same figure, in order to check the insertion loss and VSWR of the coupling structure. By terminating one such input to a 50Ω coaxial load and measuring the input VSWR, it was possible to determine whether or not the coupling was designed properly. Once this is determined, one of the inputs is closed and another sliding short is added for tuning purposes (see Figure 16). Again reference (13) can be used to easily determine the characteristic impedances of different quarter-wavelength transformers shown in Figure 16. For this reason Figure 17 is given with all the circuit parameters that were calculated.

D. Experimental Results

Experimental investigation of the amplifier in Figure 16 showed that power gains as high as 36 db at 4.72 kmc can be obtained. The frequency response of this amplifier for a particular tunnel diode is shown in Figure 18. Its 3 db bandwidth is approximately 390 mc or 8.3% at 4.72 kmc. This particular tunnel diode (MS1101) has a resistive cutoff frequency of 18 kmc.

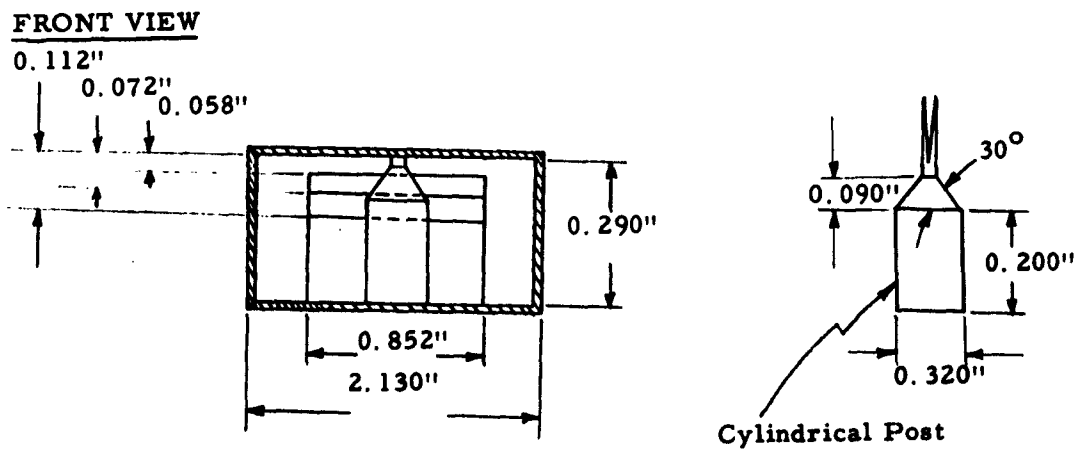
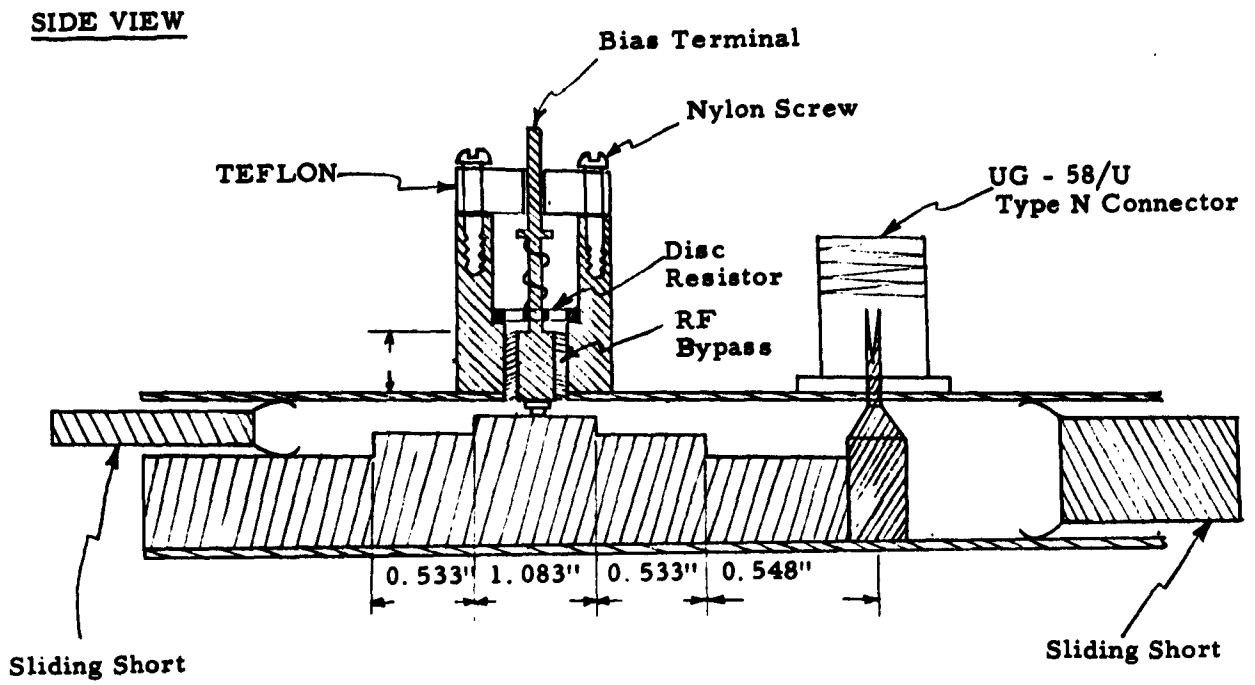


FIG. 16 CROSS-SECTIONAL VIEW OF A RIDGED-WAVEGUIDE C-BAND TUNNEL DIODE AMPLIFIER

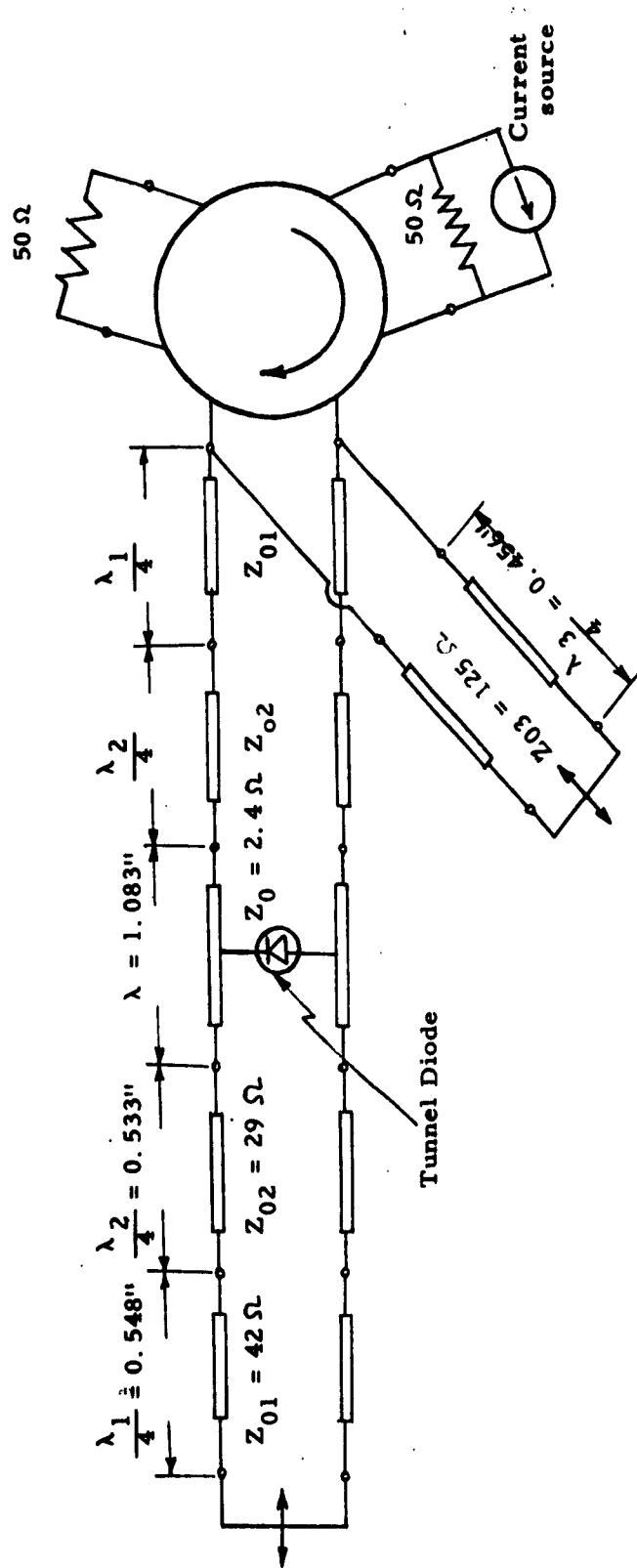


FIG.17 DIAGRAM OF A 5.65 KMC TUNNEL DIODE AMPLIFIER (DC BIASING CIRCUIT NOT SHOWN).

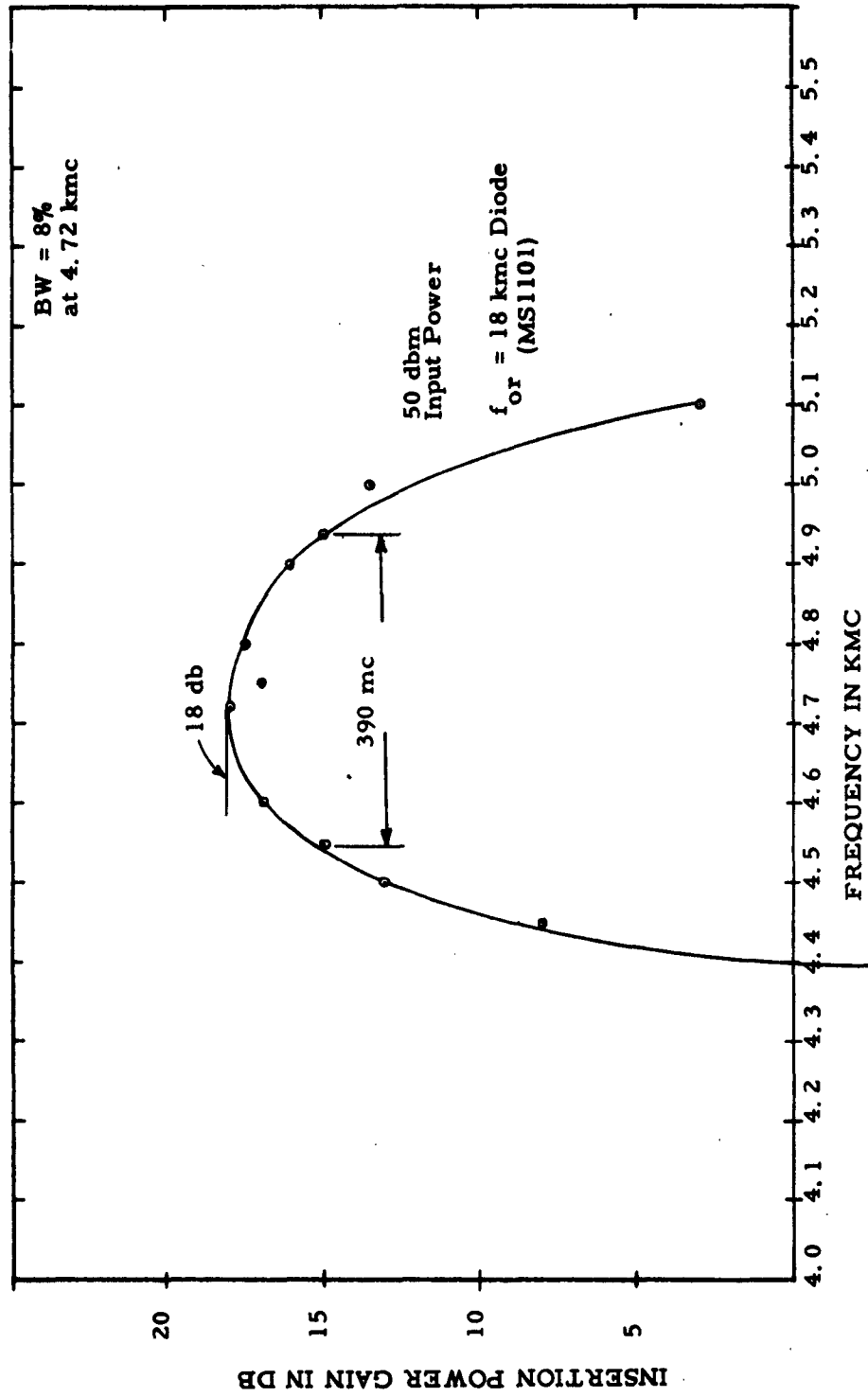


FIG.18 GAIN VERSUS FREQUENCY DIAGRAM OF TUNNEL DIODE AMPLIFIER

Other measured characteristics of the amplifier are shown in Figures 19, 20 and 21. It is of interest to note the limiting effect of the amplifier in Figure 21. The output power level of the amplifier varies only by one db when the input power decreases from 35 dbm to 60 dbm.

It was also observed that the limiting effect changed from diode to diode and by varying the D.C. bias point (see Figure 20). Note that the limiting effect is greater for higher cutoff frequency diodes. For a more complete discussion of this phenomenon and its possible application see reference 4.

However, before a complete experimental investigation could be made, a serious "burnout" problem developed. Upon placing the tunnel diodes in the RF circuit, and by trying to optimize performance of the amplifier at the desirable frequency (5.65 kmc), either by tuning or varying the d.c. bias, the tunnel diodes burned out. This unexpected difficulty did not permit any further experimental investigation of the amplifier. It is believed that transients in the dc circuit are causing this difficulty. During the next quarterly period an attempt will be made to suppress any such transients in the d.c. circuit as explained in more detail in the next section.

4. D.C. Biasing Circuit

The D.C. Biasing circuit of the 5.65 kmc tunnel diode amplifier is as shown in Figure 22. This was the actual D.C. Circuit that was used during the experimental investigation utilizing Sylvania's D4168D type tunnel diodes. The low impedance coaxial line serves as an RF by-pass capacitor for proper isolation of the RF circuit. A pyrofilm disc-type resistor is used to establish the proper load line for stability. Care was exercised to minimize

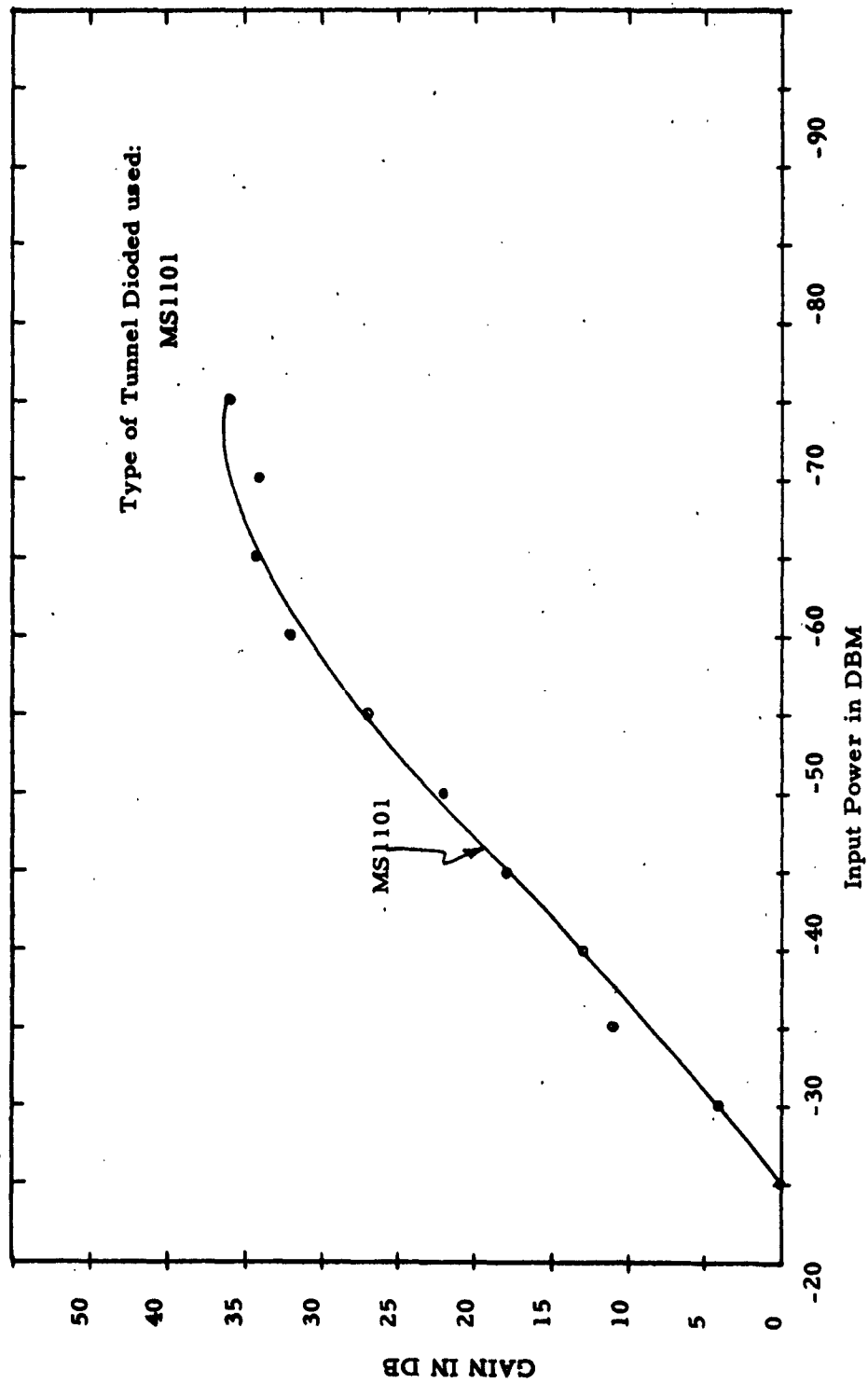


FIG. 19 GAIN VERSUS INPUT POWER DIAGRAM OF TUNNEL DIODE AMPLIFIER

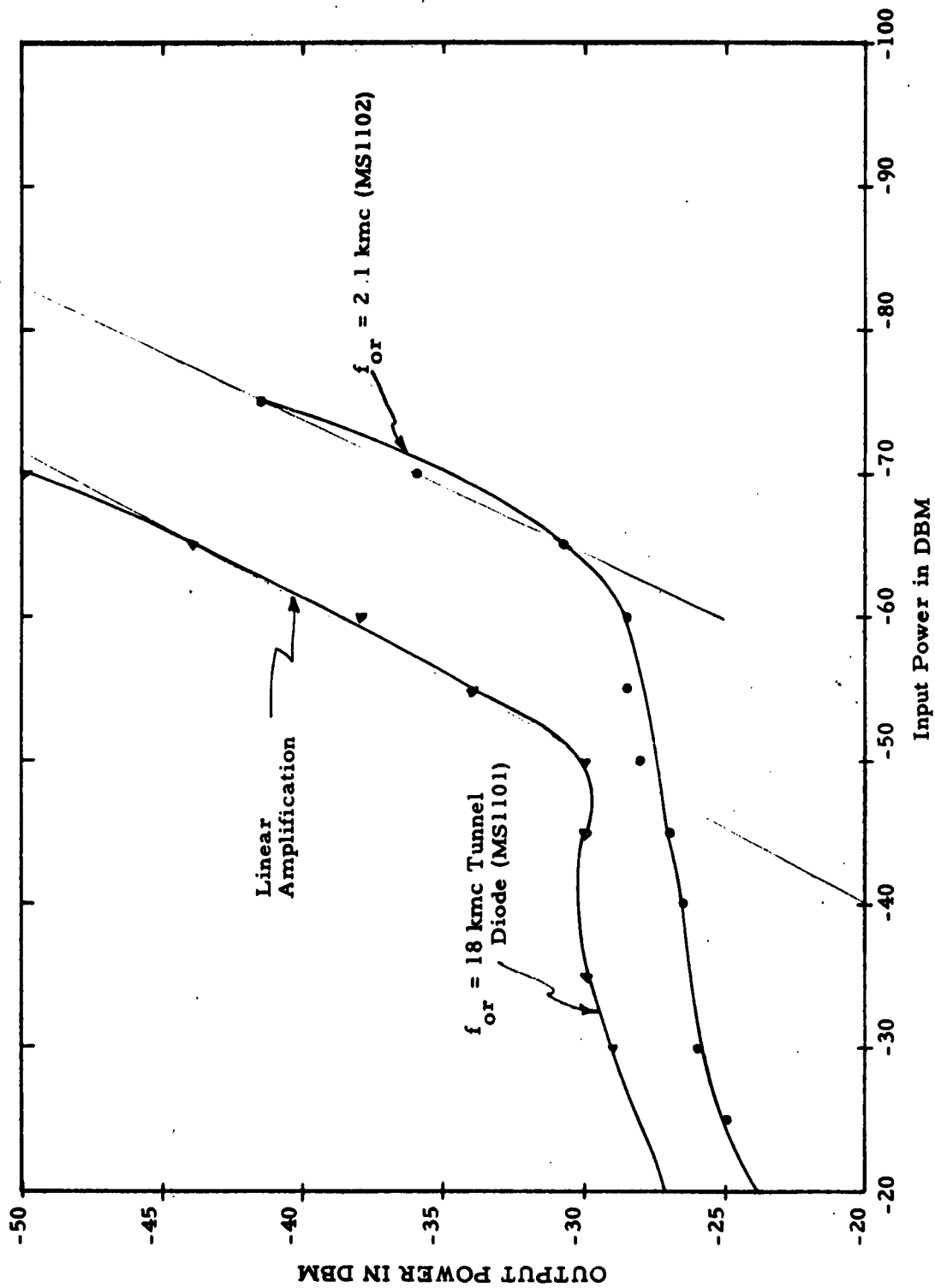


FIG. 20 DIAGRAM ILLUSTRATING RELATIVE OUTPUT POWER VERSUS INPUT POWER OF TUNNEL DIODE AMPLIFIER

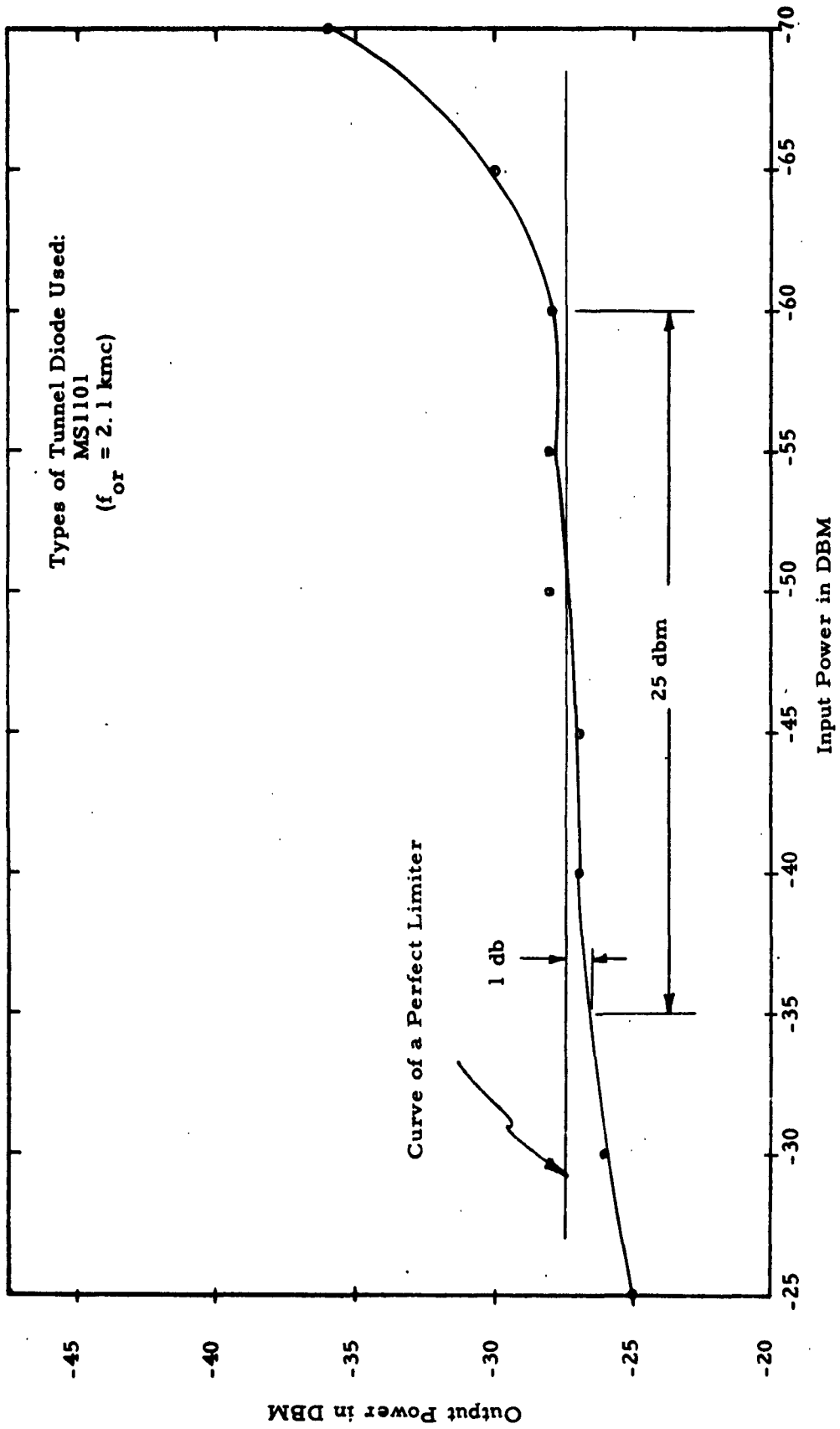


FIG. 21 DIAGRAM ILLUSTRATING RELATIVE OUTPUT POWER VS INPUT POWER OF TUNNEL DIODE AMPLIFIER

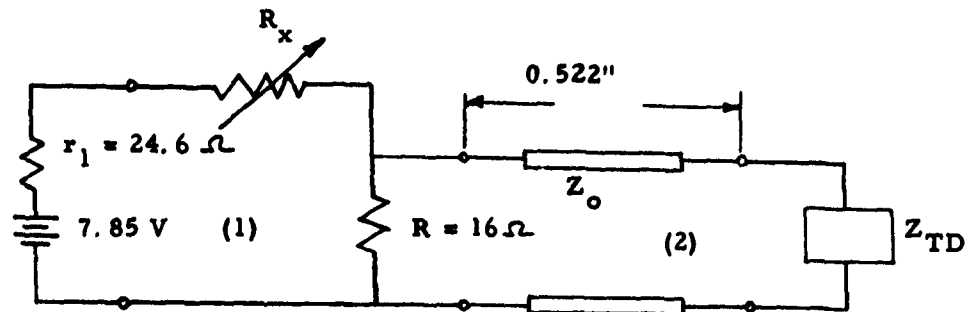


FIG. 22 D. C. BIASING CIRCUIT OF TUNNEL DIODE AMPLIFIER

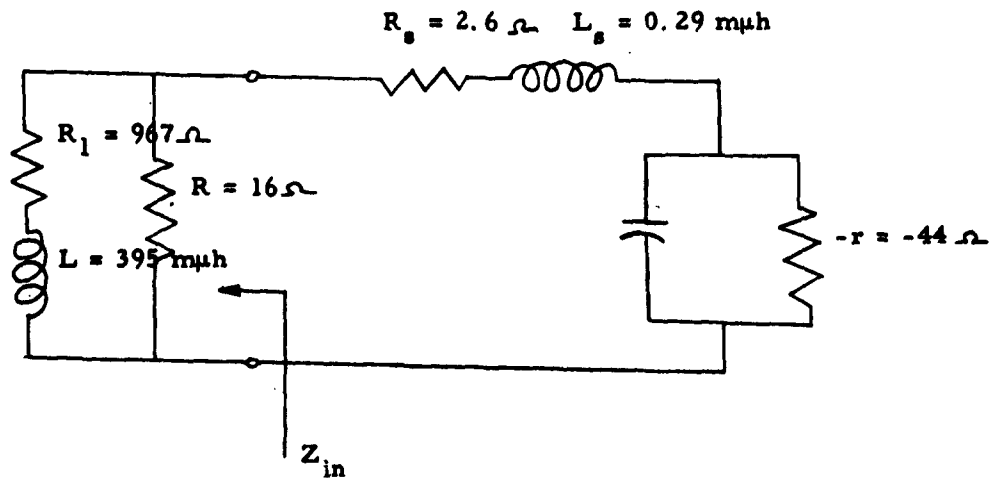


FIG. 23 D. C. BIASING CIRCUIT OF TUNNEL DIODE AMPLIFIER INCLUDING LEAD INDUCTANCE

any lead inductance hoping there would be no low frequency oscillation in the circuit which would tend to deteriorate the characteristics of the tunnel diode and eventually cause burn out. Unfortunately, a serious "burn out" problem was observed. Different types of tunnel diodes, such as Sylvania's D4168D and Micro State's Msl102 were used, and the same difficulty occurred. The entire circuit was checked and rechecked for any leakage voltage from any instrument or source, but no such voltages were present. This suggested that the problem might be due to low frequency oscillations since at high frequencies (around 5.65 kmc) the amplifier was designed to be stable.

If a more complete analysis of the D. C. circuit is carried out, it is found that low frequency oscillations do occur at approximately 570 mc. The transient analysis of the D. C. circuit in Figure 22 is formulated as follows: Since the circuit is to be examined at relatively low frequencies (below 1000 mc), the effect of the coaxial line can be neglected. It was also found by measurements and calculations that the lead inductance in loop (1), (see Figure 22) was about 395 mμh. The series resistance of the precision potentiometers used, when Sylvania's D4168D tunnel diode is biased at the operating point, was 943 ohms. Figure 23 shows the circuit including lead inductance at low frequencies.

From Figure 23

$$Z_{in}(j\omega) = R \left[\frac{R_1(R_1 + R) + (\omega L)^2}{(R_1 + R)^2 + (\omega L)^2} \right] + j\omega L \left[\frac{R^2}{(R_1 + R)^2 + (\omega L)^2} \right] \quad (55)$$

from which

$$R_{in}(\omega) = R \left[\frac{R_1(R_1 + R) + (\omega L)^2}{(R_1 + R)^2 + (\omega L)^2} \right] \quad (56)$$

and

$$X_{in}(\omega) = j\omega L_{eq} = \frac{j\omega L R^2}{(R_1 + R)^2 + (\omega L)^2} \quad (57)$$

where

$$L_{eq}(\omega) = \frac{LR^2}{(\omega L)^2 + (R_1 + R)^2} \quad (58)$$

Figure 24 shows the resultant equivalent circuit. It is well known that in order for the circuit in Figure 21 to be stable the following inequality must hold:

$$\frac{L_T(\omega)}{rC} < R_T(\omega) < r \quad (59)$$

where

$$R_T(\omega) = R_s + R_{in}(\omega) = \text{total loop resistance,}$$

$$L_T(\omega) = L_s + L_{eq}(\omega) = \text{total loop inductance.}$$

Now, using the values for the circuit parameters as shown in Figure 20,

$$R_T(\omega) = 18.6 \Omega$$

and the right hand side of inequality (59) is satisfied. Considering the left hand side of (59), it is seen that oscillations will occur when

$$\frac{L_T(\omega)}{rC} = R_T(\omega) \quad (60)$$

Calculating L_{eq} gives

$$L_{eq} = 3.4 \times 10^{-11} \text{ h}$$

which from equation (60) gives the frequency of oscillation as

$$f_{osc} = 570 \text{ mc}$$

This is the maximum frequency at which oscillations may occur because for

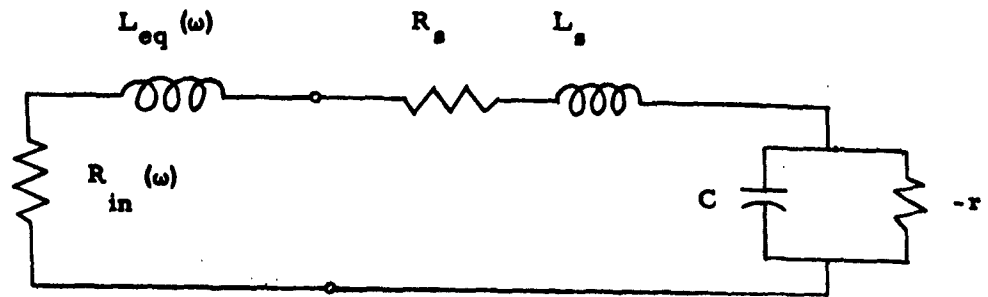


FIG. 24 EQUIVALENT D. C. BIASING CIRCUIT

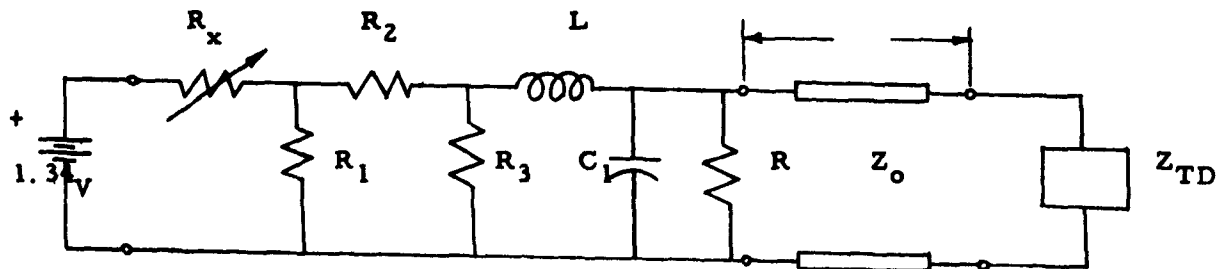


FIG. 25 MODIFIED D. C. BIASING CIRCUIT AT LOW FREQUENCIES

higher frequencies ($f > 570$ mc) $L_{eq}(\omega)$ becomes smaller and stability condition (5) is satisfied. Therefore, at any frequency below about 570 mc the D. C. circuit can oscillate, the reason being that not enough by-pass capacitance was provided for the low frequency spectrum. This condition can set up transients in the D. C. circuit which may very well cause burnout problems. It is also believed that the low frequency oscillations are of the relaxation type. On the other hand, high frequency oscillations will not introduce any problems because the by-pass is adequate.

To eliminate these problems, a modified D. C. circuit has been proposed consisting of a larger coaxial by-pass capacitor and a D. C. source which will be current limited. The modified D. C. biasing circuit to be used in the investigation of the "burnout" problem is discussed in the next section.

5. Modified Biasing Circuit

The modified D. C. biasing circuit is as shown in Figure 25. The purpose of connecting C_1 across the resistor R is to make the circuit less inductive at low frequencies so that stability maybe accomplished. At somewhat higher frequencies the coax-type capacitor will take over and stabilize the circuit. This circuit, although not completely analyzed as yet, would most certainly eliminate any oscillations by properly choosing the circuit parameters. The resistors R_1 , R_2 and R_3 , forming a π -type voltage divider is there to limit the current from the mercury cell from any changes in the negative resistance of the load as function of frequency and bias voltage.

E. Low Level Detection By Tunnel Diodes

1. Introduction

As mentioned in the first quarterly report on the project, tunnel diodes have been used by a number of investigations as low-level microwave detectors. During the past quarterly period preliminary experimentation

ARMOUR RESEARCH FOUNDATION OF ILLINOIS INSTITUTE OF TECHNOLOGY

on both tunnel diodes and backward diodes was undertaken. This section discusses the basic theory and presents the experimental results.

2. Theory

The theory of low-level diode detection is well developed in the literature. This theory can be easily extended to the tunnel and backward diodes simply by adding series inductance to the conventionally analyzed circuit. Following Torry and Whitmer a current sensitivity parameter is defined as

$$\beta = \frac{\text{short-circuit rectified current}}{\text{Absorbed RF power}} \quad (61)$$

If it is assumed that the diode is matched to the generator and that skin-effect losses are negligible, then as shown in Appendix A,

$$\beta = \frac{2KR_g R^2}{\left[(R_s + R_g - R) + \omega^2 RLC \right]^2 + \omega^2 \left[L - CR(R_s + R_g) \right]^2} \quad (62)$$

The terms in the above equation are defined in Appendix A. Note that this equation differs from that published by Montgomery. Montgomery's eqn. may be shown to be incorrect by a single dimensional argument.

Equation 62 shows that a frequency exists for which β is a maximum. β_{\max} can be shown to occur at

$$\omega_{\max} = \sqrt{\frac{1}{LC} \left(1 - \frac{R_s + R_g}{R} \right)}$$

and

$$R = \frac{L}{C(R_s + R_g)}$$

Thus ω_{\max} is the frequency at which the circuit will support steady state oscillation.

The preceding equations may be used to evaluate the sensitivity of a given diode when the diode equivalent circuit parameters are known. (Such calculations are difficult to obtain for the back diode). The above formulation does indicate that care must be employed in the design of the detector circuit to obtain maximum sensitivity. It is also interesting to note that the maximum sensitivity condition coincides with the maximum gain condition so that a circuit designed to amplify will also make a good video detector.

G. Experimental Results

The experimental results were obtained prior to the time that the above analysis was completed. The optimum circuit design was not at that time known so that pessimistic results were obtained. The technique used for the sensitivity data was the conventional tangential sensitivity measurement. The diode terminated a 50 ohm line, was by passed RF wise, and matched with a double stub tuner. Both the Sylvania tunnel diode and the Micro State MS1610 backward diode were used. The D4168D was most sensitive when biased in the negative resistance region as was expected. No bias was applied to the backward diode. Both units gave a sensitivity of the order of -40 dbm.

Future work in this area will be directed to the design of an optimum mount.

F. A Proposed Three Frequency Source Using Harmonic Generation Techniques

During a recent steering committee meeting a discussion evolved concerning the feasibility and anticipated performance of obtaining harmonic outputs of C-band and X-band from an L-band driving source. Figure 26 shows a block diagram of the required system. The system design is to be such that maximum output power be obtained while maintaining high efficiency.

ARMOUR RESEARCH FOUNDATION OF ILLINOIS INSTITUTE OF TECHNOLOGY

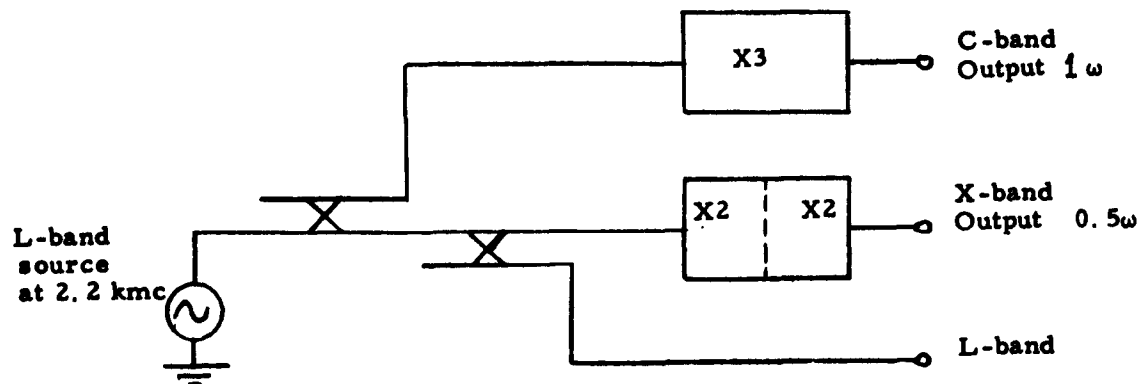


FIG. 26 TRI-BAND HARMONIC GENERATION SOURCE

size and weight are of secondary importance.

Estimation of system performance is complicated by the fact that high power output is required. Most of the present quantitative design criteria are based on a small signal analysis. This analysis fails to predict many of the experimentally observed high power effects such as saturation phenomenon, hysteresis in the input versus output power data, spurious oscillation and harmonic generation. Of particular importance regarding the proposed design is the fact that much larger efficiencies have been reported in the high power case than can be justified by the small signal analysis. One of the major contributions to increased efficiency appears to generate from driving the varactor diode into its forward conduction region. Little is presently known about this phenomenon.

For these reasons it is necessary to refer to experimental results to evaluate the proposed system. Microwave Associates have reported a doubler from 4.5 gc to 9.0 gc having a 50 percent efficiency and 700 mw output power. (It can be assumed that saturation effects or burn out restricted the maximum obtainable output power). Assuming that the L-band primary source is operating at a center frequency of 2.2 gc, it appears that doublers from 2.2 gc to 4.4 gc could also be designed with about 50 percent efficiency, triplers from 2.2 gc to 6.6 gc with 35 percent efficiency, and two cascaded doublers with an output at 8.8 gc with 25 percent efficiency. The maximum output power at C-band would be of the order of 1 watt with 0.5 watts at X-band.

The L-band source to use has not yet been decided upon. Based on the above, about 15 watts of drive power is required.

It is recommended that work be undertaken to develop the above system.

G. Electronically Tunable Tunnel Diode Oscillator

During the past quarterly period some effort has been devoted to the design of a C-band electronically tunable tunnel diode oscillator. The circuit under study is shown in Figure 27. Only one reference on this type of design has been found in the literature. The cited reference contains only a qualitative discussion of the design concept. The quantitative analysis of the circuit is as yet uncompleted. Work in this area will continue during the next quarterly period.

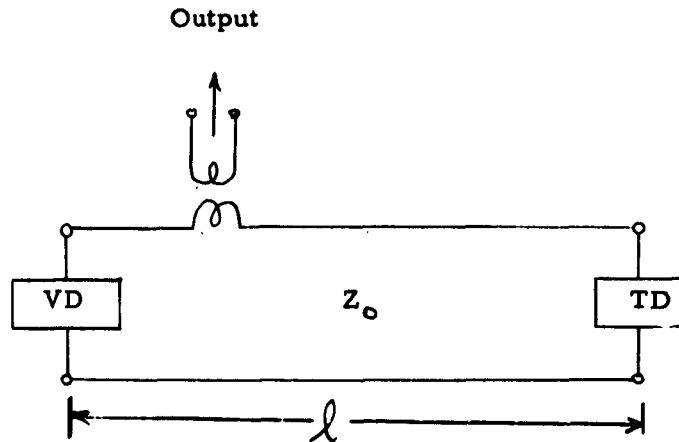


FIG. 27 SCHEMATIC OF VARACTOR TUNABLE TUNNEL DIODE OSCILLATOR

H. 1. Doppler Tracking Errors Due to Frequency Instability of the Tracking Loop Voltage Controlled Oscillator

Modification of the AN/FPS-16 tracking radar to perform coherent Doppler tracking has resulted in data indicating that frequency instability of the VCO (voltage-controlled oscillator) in the radar Doppler tracking loop may be a limiting factor in the achievement of accurate velocity data.¹⁵ The following section analyzes this source of noise on a theoretical basis.

The fundamental source of frequency error in oscillators arises from phase perturbations caused by the shot and thermal noise inherent in the device. Although the phase perturbations are random, the phase error will tend to build-up over a period of time. Consider the actual VCO (voltage-controlled oscillator) as an ideal VCO and a noise source. Suppose the noise source produces white noise which is fed into the input of the VCO. From Bendat¹⁶ the total mean square phase perturbations at the system output produced by a spectral density of white noise, η , at the input and measured over a period of time, τ , is given by the expression:

$$\sigma^2(\tau) = \eta/2 \int_0^\tau h^2(t) dt \quad (63)$$

where $h(t)$ is the weighting function of the system. The VCO phase output is the integral of its instantaneous frequency, corresponding to a weighting function, $h(t)$, of unity. Hence, the total mean square phase perturbation produced by the white noise spectral density is given by:

$$\sigma^2(\tau) = \eta/2 \int_0^\tau dt = \frac{\eta}{2} \tau \quad (64)$$

Thus, the total amount of mean square phase perturbation is directly proportional to the time elapsed and to the input spectral density. The phase-error buildup of an oscillator has been shown by Edson¹⁷ to be

$$\sigma^2(\tau) = \tau / \tau_c \quad (65)$$

where τ_c , the "period of coherence", is the time required for the rms error to reach one radian. Eq. (65) has the same form as (64), indicating that the assumption of a "white noise" equivalent for the f-m noise modulation is correct. Combining (64) and (65) gives the relation between η and τ_c :

$$\eta = 2/\tau_c \quad (66)$$

4. Tracking Loop

The doppler tracking loop is presented in block diagram form in Figure 28 . There are two modes of operation, narrow band- ± 16 cps- and wide band ± 50 cps-centered around the carrier. The two fine line bandpass filters are identical symmetric two pole filters with 180° of phase shift across the pass band. It is shown in appendix B that the band pass characteristic of a symmetric filter acts as a low pass filter on the modulation of a narrow band FM signal. Therefore, the band pass filters preceding the discriminator can be replaced by equivalent low pass filters following the discriminator. The transfer function of each filter is given by the expression:

$$Y_f(j\omega) = \frac{1}{(1 + j\omega T_1)^2} \quad (67)$$

Since the pass band is here defined as that bandwidth over which the phase shift is 180° , there will be 90° of phase shift across the pass band of the equivalent low pass filter. The value of the time constant, T_1 , is determined by setting the phase shift characteristic equal to $\pi/2$ at a frequency ω_B , the bandwidth of the low pass filter:

$$-\pi/2 = -2 \tan^{-1} \omega_B T_1 \quad (68)$$

solving (68) for the time constant,

$$T_1 = 1/\omega_B \quad (68a)$$

For narrow band operation, (16 cps) T_1 is $(2\pi (16))^{-1}$ and for wide band operation (50 cps) T_1 is $(2\pi (50))^{-1}$. The discriminator is assumed to operate ideally with transfer function, K_D , of $25 \times 10^{-3}/2\pi$ volts per radian per second. The first integrator has a transfer function

$$Y_{I_1}(j\omega) = -K_{I_1}/j\omega \quad (69)$$

where K_{I_1} is 100/sec for narrow band operation and 200/sec for wide band operation. The second integrator has a transfer function

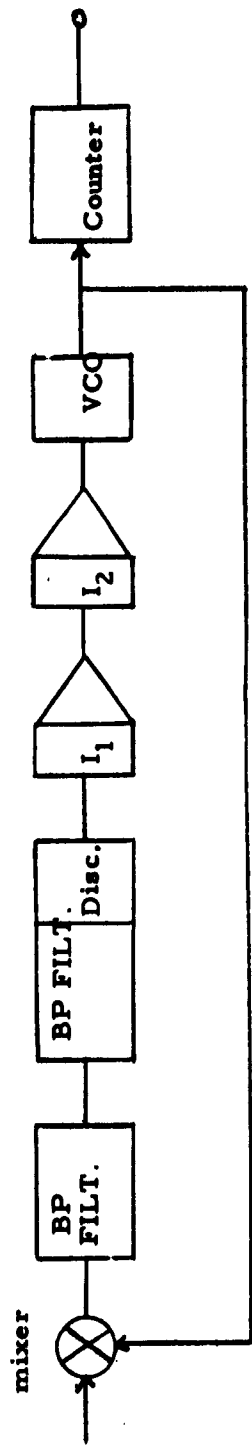


FIG. 28a BLOCK DIAGRAM

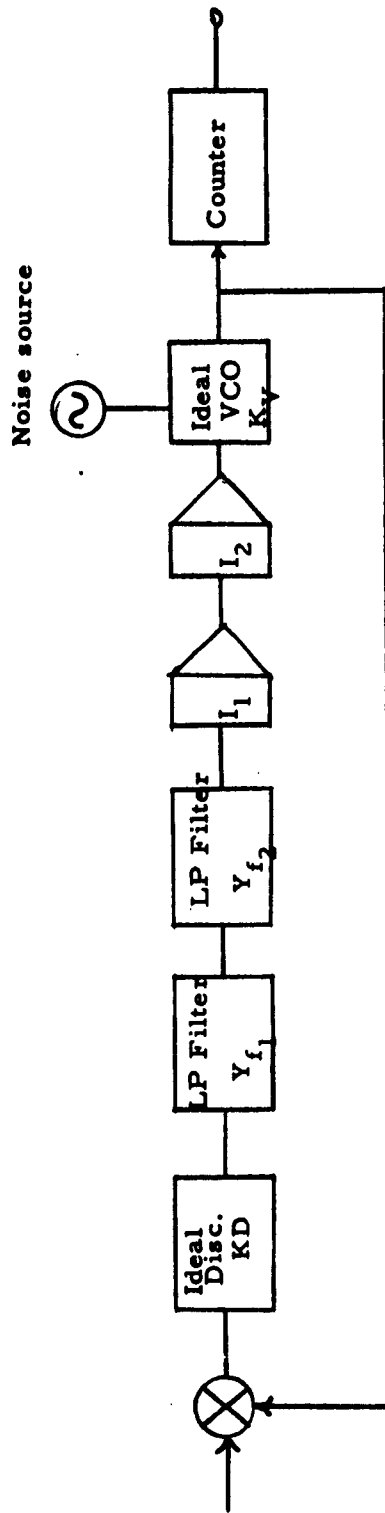


FIG. 28b REVISED BLOCK DIAGRAM

$$Y_{I_1}(j\omega) = -K_{I_2}/j\omega \quad (70)$$

for which K_{I_2} is 1/sec for narrow band operation and 3/sec for wide band operation. The VCO can be represented as an ideal VCO and a source of white noise. The transfer function of the VCO, K_V , is a constant $2\pi \times 10^4$ radians per second per volt. \mathcal{N} , radians per second $((\text{rad/sec})^2/\text{rad/sec})$ is the input power spectral density.*

To determine the frequency error introduced by the noise in the VCO, the transfer function from the VCO to the normal loop output must be derived. The input signal at the VCO consists of the input signal from the noise source, e_N and the feedback component of the loop, e_L :

$$e_{IN} = e_N + e_L \quad (71)$$

The feedback component is determined by tracing through the loop. At the mixer output (assuming a constant frequency input, e_f , at the normal loop input) the signal is

$$e_\omega = e_f - e_o \quad (72)$$

This signal, e_ω , is then modified by the other components of the loop to obtain e_L :

$$e_L = e_\omega K_D Y_{f_1} Y_{f_2} Y_{I_1} Y_{I_2} \quad (73)$$

The output signal fed to the counter is the input signal modified by the VCO transfer function.

$$\begin{aligned} e_o &= K_V e_{IN} \\ &= K_V [e_N + e_L] = K_V [e_N + (e_f - e_o) Y_D Y_{f_1} Y_{f_2} Y_{I_1} Y_{I_2}] \\ &= K_V e_N + e_f Y(j\omega) - e_o Y_j(\omega) \end{aligned} \quad (74)$$

ARMOUR RESEARCH FOUNDATION OF ILLINOIS INSTITUTE OF TECHNOLOGY
* Since the loop tracks frequency rather than voltage, loop noise density is in terms of $(\text{frequency})^2$ per unit bandwidth rather than $(\text{volts})^2$ per unit bandwidth; i. e., $(\text{rad/sec})^2/(\text{rad/sec}) = \text{rad/sec}$.

Simplifying (74) gives:

$$e_o = \frac{K_V e_N}{1 + Y(j\omega)} - \frac{e_f Y(j\omega)}{1 + Y(j\omega)} \quad (75)$$

Since the error due to noise is of prime concern only the transfer function for the noise component will be considered. The transfer function of the loop for the noise component is:

$$H_N(j\omega) = \frac{K_V}{1 + Y(j\omega)} \quad (76)$$

where $Y(j\omega)$ is the combined transfer function of the various components or symbolically

$$\begin{aligned} Y(j\omega) &= K_D K_V Y_{f_1} Y_{f_2} Y_{I_1} Y_{I_2} \\ &= K_D K_V K_{I_1} K_{I_2} / -\omega^2 (1 + j\omega T_1)^4 \\ &= K / -\omega^2 (1 + j\omega T_1)^4. \end{aligned} \quad (77)$$

Substitution of equation (77) into equation (76) reduces the loop transfer function for noise error to the expression:

$$H_N(j\omega) = - \frac{K_V \omega^2 (1 + j\omega T_1)^4}{K - \omega^2 (1 + j\omega T_1)^4} \quad (78)$$

The output spectral density η_o is the product of the input spectral density η and the absolute value squared of the system transfer function

$H_N(j\omega)$:

$$\eta_o = \eta |H_N(j\omega)|^2. \quad (79)$$

A counter at the VCO output measures the frequency in time intervals T , of 0.1 second. The counter output is actually the mean value of the instantaneous frequencies fed into it during the counting interval. Hence,

the counter has a weighting function (or impulse response_ in the time domain of

$$f(t) = \begin{cases} \frac{1}{T} & 0 \leq t \leq T \\ 0 & t > T \end{cases} \quad (80)$$

The transfer function corresponding to (80) is

$$H_c(j\omega) = e^{-j\frac{\omega T}{2}} \frac{\sin \frac{\omega T}{2}}{\frac{\omega T}{2}} \quad (81)$$

and the power transfer function is

$$\left| H_c(j\omega) \right|^2 = \left| \frac{\sin \frac{\omega T}{2}}{\frac{\omega T}{2}} \right|^2 \quad (82)$$

Since white noise is the input to the VCO all values of frequency may exist at the counter input. Thus, the total mean square frequency error will be the sum of the contributions from each frequency. This is expressed in mathematical form by the equation:

$$\begin{aligned} \epsilon^2 &= \eta \int_0^{\infty} \left| H_c(j\omega) \right|^2 \left| H_N(j\omega) \right|^2 d\omega \\ \text{or} \\ &= \eta K_V^2 \int_0^{\infty} \left| \frac{\sin \frac{\omega T}{2}}{\frac{\omega T}{2}} \right|^2 \left| \frac{\omega^2 (1 + j\omega T_1)^4}{K - \omega^2 (1 + j\omega T_1)^4} \right|^2 d\omega. \end{aligned} \quad (83)$$

Because of the difficulty in evaluating the above integral, the approximation

$$\left| H_c(j\omega) \right|^2 = \left| \frac{1}{1 + j\omega T/2} \right|^2 \quad (84)$$

will be used. The validity of this approximation is discussed in Appendix C. With this approximation the mean square error may be determined by a method outlined in the "Theory of Servomechanisms."¹⁸ This technique is for the

evaluation of integrals of the form

$$I_n = \frac{1}{2\pi j} \int_{-\infty}^{\infty} \frac{g_n(x)}{h_n(x) h_n(-x)} dx \quad (85)$$

where $g_n(x)$ is the polynomial

$$g_n(x) = b_0 x^{2n-2} + b_1 x^{2n-4} + \dots + b_{n-1} \quad (86)$$

and $h_n(x)$ is the polynomial

$$h_n(x) = a_0 x^n + a_1 x^{n-1} + \dots + a_n \quad (87)$$

Substituting equation (84) into (83) and making the substitutions $\omega T_1 = x$, $a = T/2T_1$, and $T_1^2 K = D$ reduces the expression for the mean square error to

$$\epsilon^2 = \eta \frac{K_V^2}{T_1} \int_0^{\infty} \frac{x^4 [1+x^2]^4 dx}{(1+jax)(D-x^2(1+jx)^4)(D-x^2(1-jx)^4)(1-jax)} \quad (88)$$

which can easily be expanded to the form of equation (81)

Evaluating (81) according to the method in "Theory of Servomechanisms", the mean square error in general form is

$$\begin{aligned} \epsilon^2 = \frac{\eta K_V^2 (-1)^\pi}{T} & \left[16a^5 D^2 + D(384a^6 + 1216a^5 + 1268a^4 + 226a^3 + 76a^2 + 144a - 64) \right. \\ & \left. + 16a^5 - 72a^4 + 188a^3 + 608a^2 - 960a - 512 \right] / \\ & \left[a^3 D^2 (532a^2 + 396a + 222) + D(-448a^6 + 176a^5 + \right. \\ & \left. 1268a^4 - 580a^3 - 130a^2 - 24a) - 384a^4 - 1935a^3 + 278a^2 \right. \\ & \left. + 2256a - 320 \right]. \quad (89) \end{aligned}$$

For the narrow band mode, $a \approx 5$, and $D \approx 2.5$, the mean square error is

$$\begin{aligned} \epsilon^2 &= \frac{\pi \eta K_V^2}{T} \times 10 = 4\pi^3 \eta 10^9 \times 10 \text{ (rad/sec)}^2 \quad (90) \\ &= \eta 10^9 \times 10 \text{ (cps)}^2. \end{aligned}$$

For the wide band mode, $a = 5\pi$, and $D \approx 1.5$, the mean square error is

$$\begin{aligned} \epsilon^2 &= \frac{\pi \eta K_V^2}{T} (1.24) = 4\pi^3 \eta (1.24) 10^9 (\text{rad/sec})^2 & (91) \\ &= \pi \eta 10^9 \times (1.24) (\text{cps})^2 \end{aligned}$$

a comparison of (90) and (91) show that the noise error is larger in the narrow band mode, in agreement with experiment.

Typical values of rms frequency error, as reported by RCA, are 2.88 cps for the wide band mode and 5.04 cps for the narrow band mode. These values are from data taken with the loop tracking on the central spectral line for an internally generated signal. The ratio of narrow band mean square error to wide band mean square error is 3.04 for the above experimental values and 8.06 for the theoretical values. The discrepancy in the theoretical and experimental ratios may be due to additional sources of noise in the actual equipment.

III. CONCLUSIONS

During the past quarterly period a review of tunnel diode amplifier theory has been conducted. The available analyses have been considered in view of the practical limitations imposed by the respective restrictive assumptions placed on them. Experimental work has been conducted on C-band amplifiers. This work indicates that serious consideration must be given to the biasing circuit design so as to avoid possible transient effects which might cause diode burn out.

A theoretical analysis of the response of a Doppler tracking loop to VCO frequency errors has been performed. It is shown that the maximum error results in the narrowband mode, in agreement with experimental results. However, the increase in noise in the wideband mode is less in the experimental data than theory would predict, indicating the presence of additional noise sources other than VCO noise.

Respectfully submitted,



R. D. Standley, Research Engineer

APPROVED:

J. T. Ludwig, Acting Manager
Microwaves, Antennas and Propagation

J. E. McManus, Assistant Director
Electronics Research

IV. PROGRAM FOR NEXT INTERVAL

The following areas will be investigated during the next quarterly period:

- 1) The synthesis problem will be further considered.
- 2) The modified dc biasing circuit will be analyzed.
- 3) Experimental C-band amplifier work will be continued.
- 4) A near optimum tunnel diode video detector will be designed.

V. IDENTIFICATION OF PERSONNEL

The following personnel have contributed to work herein reported during the past quarterly:

J. Ludwig, Manager, Research Engineer	112 hours
S. Kazel, Research Engineer	232 hours
R. Standley, Research Engineer	228 hours
P. Toullos, Assistant Engineer	456 hours
J. Feldman, Assistant Engineer	274 hours

The biography of each of the above individuals appears in the following pages.

LUDWIG, JOHN T.

TITLE:

Research Engineer; Acting Manager

PRINCIPAL FIELDS:

Microwaves and Magnetics

EXPERIENCE:

Before coming to Armour Research Foundation, Dr. Ludwig, has had fourteen years of professional experience including theoretical and experimental microwave and UHF studies, magnetic device studies, acoustic studies, exotic gyroscope developments.

He has made studies of UHF scatter-diffraction propagation over rough terrain and UHF high power generation. Other areas of effort have included information and communication theory, electronic instrumentation of physical measurements and wide-band magnetic tape recording.

TECHNICAL PAPERS:

'Multiple Operation of Reflex Klystrons in an Annular Cavity' April 1952, Master of Science Thesis, University of Minnesota

"Research and Development on Design Method for Reactors", Six Quarterly Reports dated December 15, 1952 through March 15, 1954, and "Final Report", September 1954. University of Minnesota. Contract No. DA 36-039 SC-42573, Report ASTIA numbers AD-3817, -9558, -20383, -22613, -32983, -31759, and -64525, Final.

"A Study in the Design of Magnetic Circuits Employing Soft Magnetic Materials and Superposed A-C and D-C Magnetization," June 1954, Doctor of Philosophy Thesis, University of Minnesota.

"A New Method for Inductor Design", Proceedings of Electronic Components Conference, pp. 18-21 May 1955, Los Angeles.

"Design of Optimum Inductors Using Magnetically Hard Ferrites in Combination with Magnetically Soft Materials". Journal of Applied Physics, Vol. 29, pp. 497-499, March 1958, Presented at 1957 Conference on Magnetism and Magnetic Materials.

LUDWIG, JOHN, T. (Con, d)

"Designing Optimum Inductors with Ferrite-Biased Gaps", Electrical Manufacturing, Vol. 63, No. 1, pp. 78-90, 204, 206, Jan. 1959

"Inductors Biased with Permanent Magnets: Part II--Theory and Analysis", 60-198, Transactions AIEE, Part I., Vol. 79, pp. 273-278, 1960, Also Communications and Electronics, No. 49, July 1960.

"Inductors Biased with Permanent Magnets: Part II--Design and Synthesis", 60-199, Transactions AIEE, Part I, Vol. 79, pp. 278-291, 1960, also Communications and Electronics, No. 49, July 1960. This paper was awarded the 1959-60 AIEE Great Lakes District Second Prize.

"A Method for the Design of Holding Electromagnets", 60-197, Transactions AIEE, Part I, Vol. 79, pp. 300-310, 1960, Also, Communications and Electronics, No. 49, July 1960.

"Inductors Biased with Permanent Magnets", (Digest) Electrical Engineering, Vol. 80, p. 408, June 1961.

"A Method for the Design of Holding Electromagnets", (Digest) Electrical Engineering, Vol. 80, p. 503, July 1961.

EDUCATION:

B. E. E. with Distinction,
University of Minnesota, 1948

M.S. in E. E. University of Minnesota, 1952

Ph. D. University of Minnesota, 1954.

Numerous other courses including,
Magnetohydrodynamics Honorary Fellowship,
University of Minnesota 1959

AFFILIATIONS:

Member, American Association for the
Advancement of Science

Member, Eta Kappa Nu

Senior Member, IEEE(AIEE-IRE), 1962 Patron
Award, Florida West Coast Section (IRE)

ARMOUR RESEARCH FOUNDATION OF ILLINOIS INSTITUTE OF TECHNOLOGY

LUDWIG, JOHN T.

Professional Engineer Member, National Society of Professional Engineers (Several local and state offices and national committees)

Listing, National Engineers Register, Finder's List

Listing, Leaders in American Science

Registered Professional Engineer, Illinois Minnesota and Florida

KAZEL, SIDNEY

TITLE:

Research Engineer

PRINCIPAL FIELD:

Communications and Radar

EXPERIENCE:

Mr. Kazel has worked for eight years in the field of radar and communication theory, in the following assignments:

- (1) Participated in the development of a CW-Doppler radar for vector miss-distance indication.
- (2) Analysis of techniques for bandwidth reduction of television signals.
- (3) Analysis of the reduction in channel capacity of a fading communication link in the presence of a fading jamming signal.
- (4) Member, Advisory Committee on Radio Countermeasures, Project Monmouth II.
- (5) Development of a radio technique for unambiguous determination of missile roll orientation.
- (6) Determination optimum parameters of pulse modulation methods under conditions of limited duty cycle, for use in radar command.
- (7) System design of a highly secure command receiver for radar command of missiles.
- (8) Analysis and optimization of the factors affecting the performance of radar-beacon tracking systems.
- (9) Determination of optimum search radar techniques for early detection of ballistic missiles.
- (10) Application of the theory of optimum linear prediction and filtering to determine the theoretical improvement in radar tracking accuracy result from coherent operation.
- (11) Determination of a method for accurate angular location of deep space probes, using Doppler measurements only.
- (12) Analysis of the spreading of the spectrum of the Doppler signal in two-way Doppler systems, due to inherent oscillator instabilities.
- (13) Analysis of optimum parameters and performance characteristics of a coherent radar-beacon.
- (14) Development of a beacon antenna system with automatically controlled directivity.

TECHNICAL PAPERS:

- (1) "A Study of Video Bandwidth Compression Techniques", co-authored with J. E. Kietzer, H. M. Sachs, and H. Zucker, Proceedings of the Magnetic Recording Technical Meeting, Armour Research Foundation, Chicago, Illinois, Oct. 4-5, 1956.

KAZEL, SIDNEY (Con'd)

(2) "Comparison of PPM and PCM for Radar Command", Proceedings of the National Symposium on Telemetry, Miami Beach, Fla. Sept. 22-24, 1958.

(3) "Optimum Parameters of Pulse Modulation Systems", Section Meeting of the Professional Group on Telemetry and Remote Control, Chicago, Illinois, Oct. 1959.

(4) "Improvement in Tracking Accuracy of Pulse Radar by Coherent Techniques", co-authored with J. N. Faraone, IRE Transactions on Military Electronics, Oct. 1961.

(5) "Spectrum Broadening Due to Frequency Instability in a Two-Way Coherent Doppler System", (Accepted for publication in the Proceedings of the IRE).

EDUCATION:

B.A. in Liberal Arts, University of Chicago, 1950
B.S. in E.E., Illinois Institute of Technology, 1953
M.S. in E.E., Stanford University, 1954

AFFILIATIONS:

Institute of Radio Engineers
Tau Beta Pi (Engineering)
Eta Kappa Nu (Electrical Engineering)

STANDLEY, ROBERT D.

TITLE:

Research Engineer

PRINCIPAL FIELD:

Microwave Components

EXPERIENCE:

Mr. Standley has had five years experience in the area of microwave component theory and design. During his three years in the Microwave and Electromechanical Branch at the U. S. Army Research and Development Laboratory, Ft. Monmouth, N. J., he was Project Engineer for programs involving research and development of microwave filters, polarization converters, and directional couplers. His experience in microwave filter design includes the development of numerous band pass filters in the frequency range 1 kmc to 24 kmc which required coax, strip line, and rectangular waveguide. He has also developed C- and K-band wide stop band filters, L, S, and S-band directional filters, and S- and X-band, band rejection filters. He has pursued research in the area of electronic tuning by means of varactor diodes.

Since joining Armour Research Foundation, Mr. Standley has worked on parametric amplifiers (both regenerative and super-regenerative), tunnel diode amplifiers, ferrite circulators, electronically tunable filters, broadband hybrids (X and Ku bands), and diplexer networks.

TECHNICAL PAPER:

"A C-Band Super-Regenerative Detector for Radar Beacon Applications", Proceedings of NEC, Vol. 17, pp. 490-499, October 1961.

EDUCATION:

B. S in E. E., 1957, University of Illinois
M. S. in E. E., 1960, Rutgers University
Currently pursuing Ph. D Program at I. I. T.

AFFILIATIONS:

Member of IEEE(IRE), Chairman Chicago
Section of PGMTT, 1961-1962
Sigma Tau
Sigma Xi

TOULIOS, PETER P.

TITLE:

Assistant Engineer

PRINCIPAL FIELD:

Microwaves, Antennas and Propagation

EXPERIENCE:

Mr. Toullos has had two years of experience in the area of microwave theory and design. His experience in microwaves includes research and development of electronically tunable S-band band-pass filters using yttrium iron garnet crystals. He has also been involved on a program dealing with the determination of the state-of-the-art of VLF and HF antenna techniques and the development of VLF antennas.

Since joining Armour Research Foundation, Mr. Toullos has been concerned with the applicability of parametric and tunnel diode amplifiers to radar beacon receiver design. He has recently worked on the design and development of S, C, and X-band tunnel diode amplifiers, oscillators, and power limiters.

EDUCATION:

**B.S. in E.E., 1960, University of Illinois
M.S. in E.E., 1961, University of Illinois
Currently pursuing work leading to a
Ph.D at Illinois Institute of Technology**

AFFILIATIONS:

Member of IEEE(IRE) and PGMTT, PGCT

FELDMAN, JUDITH R.

TITLE:

Assistant Engineer

PRINCIPAL FIELD:

Communications and Radar

EXPERIENCE:

Miss Feldman joined the Foundation in June 1959, and has participated in various programs concerning communication systems and radar. This includes a study of general noise theory and application of the theory to the solution of detection problems for amplitude and pulse modulation; the use of carrier tones to transmit digital data including an investigation of optimum filtering techniques, and the effects of Gaussian noise, impulse noise, and transmission line characteristics on the received signals. Miss Feldman has also worked on transistor circuit development for a wideband spectrum analysis device and on the factors affecting high altitude radio interference instrumentation. At present, she is concerned with the use of radar to observe and measure meteorological phenomena and with a foundation sponsored program on detection theory. As an undergraduate, Miss Feldman worked as an engineering assistant and technician in the manufacture of resistive and semiconductor components.

EDUCATION:

B.S. in E. E., Illinois Institute of Technology,
1959
M.S. in E. E., Illinois Institute of Technology,
1962

TECHNICAL PAPERS:

"An Analysis of Frequency Shift Keying Systems", co-authored with J.N. Faraone, National Electronics Conference, October 1961.

AFFILIATIONS:

Institute of Radio Engineers
American Institute of Electrical Engineers
National Society of Professional Engineers
AAAS

APPENDIX A

DERIVATION OF THE CURRENT SENSITIVITY PARAMETER β

ARMOUR RESEARCH FOUNDATION OF ILLINOIS INSTITUTE OF TECHNOLOGY

APPENDIX A

DERIVATION OF THE CURRENT SENSITIVITY PARAMETER β

The current sensitivity parameter may be defined as

$$\beta = \frac{\text{short circuited rectified current}}{\text{available rf power}}$$

$$\beta = \frac{I_{dc}}{P \text{ available}}$$

To find I_{dc} , the voltage across R, V_R must be known in terms of V_g , A_n analysis of the circuit shown in Figure A shows that

$$V_R^2 = \frac{V_g^2 R^2}{[(R_g + R_s - R) + \omega^2 RLC]^2 + \omega^2 [L - CR(R_s + R_g)]^2}$$

If it is assumed that the diode is square-law then

$$I_{dc} = K V_R^2 \text{ so that}$$

$$\beta = \frac{K V_R^2}{V_g^2 / 4R_g} = \frac{4 K R_g R^2}{[(R_g + R_s - R) + \omega^2 RLC]^2 + \omega^2 [L - CR(R_s + R_g)]^2}$$

Now $\beta \rightarrow \infty$ as the denominator approaches zero. This happens when

$$R = \frac{L}{C(R_s + R_g)}$$

$$\omega_{max} = \sqrt{\frac{1}{LC} \left(\frac{R_g + R_s}{R} - 1 \right)}$$

But these two conditions are those necessary for steady state oscillation at ω_{\max} . Thus maximum sensitivity implies that the circuit is adjusted to near oscillation, i. e. an optimum mount design exists.

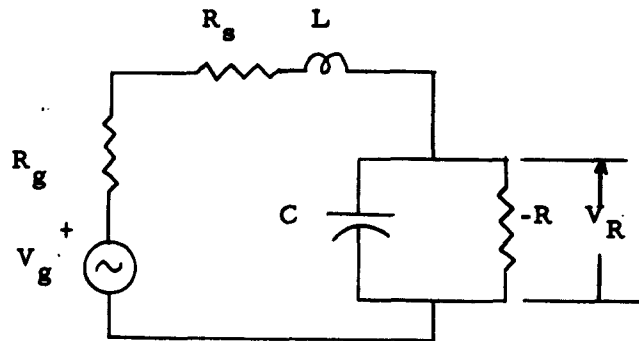


FIGURE A: TUNNEL DIODE DETECTOR CIRCUIT

APPENDIX B

TO SHOW THAT THE BANDPASS CHARACTERISTIC OF A SYMMETRIC FILTER
ACTS AS A LOW PASS FILTER ON THE MODULATION OF A NARROW BAND
FM SIGNAL

ARMOUR RESEARCH FOUNDATION OF ILLINOIS INSTITUTE OF TECHNOLOGY

APPENDIX B

TO SHOW THAT THE BANDPASS CHARACTERISTIC OF A SYMMETRIC FILTER ACTS AS A LOW PASS FILTER ON THE MODULATION OF A NARROW BAND FM SIGNAL

Under normal tracking conditions, the VCO frequency will track the loop input frequency closely, resulting in a low deviation narrow band signal into the band pass filter. A narrow band fm signal has only two significant sidebands and hence can be expressed as

$$F(t) = a_0 \cos \omega_c t + a_1 \cos (\omega_c t + \phi + \pi/2) + a_1 \cos (\omega_c t - \phi \pi/2) \quad (B-1)$$

with vectoral representation as in figure



FIG. B-1

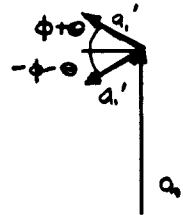


FIG. B-2

The band pass filter will reduce the magnitude of the sidebands relative to the carrier, and shift their phase as pictured in figure B-2. Or mathematically, the output of the bandpass filter for the input of a narrow band fm signal is

$$F_1(t) = a_0' \cos \omega_c t + a_1' \cos (\omega_c t + \phi + \theta + \pi/2) + a_1' \cos (\omega_c t - \phi - \theta + \pi/2). \quad (B-2)$$

Passing $F_1(t)$ through a discriminator results in a signal of the form

$$F_2(t) = a_1'' \sin (\theta + \phi) \quad (B-3)$$

This is equivalent to passing the narrow band fm signal through the discriminator and then through a low pass filter with some characteristic as the bandpass filter centered at zero frequency. Thus, the bandpass characteristic of a symmetric filter acts as a low pass filter on the modulation component of a narrow-band FM signal.

APPENDIX C

LOW PASS FILTER APPROXIMATION TO THE COUNTER CHARACTERISTIC

ARMOUR RESEARCH FOUNDATION OF ILLINOIS INSTITUTE OF TECHNOLOGY

APPENDIX C

LOW PASS FILTER APPROXIMATION TO THE COUNTER CHARACTERISTIC

The counter transfer function is given by

$$\left| H_c(j\omega) \right|^2 = \left| \frac{\sin \frac{\omega T}{2}}{\frac{\omega T}{2}} \right|^2 \quad (82)$$

A low pass filter with transfer function

$$\left| H_L(j\omega) \right|^2 = \left| \frac{1}{1 + j\omega \zeta} \right|^2 \quad (C-1)$$

will have equal area over-all frequencies if $\zeta = T/2$. This is shown by computing the area under both curves. Thus,

$$A_c = \int_0^{\infty} \frac{\sin^2 \frac{\omega T}{2}}{\frac{\omega T}{2}} d\omega = \pi/1 \quad (C-2)$$

and

$$A_L = \int_0^{\infty} \frac{1}{1 + \omega^2 \zeta^2} d\omega = \pi/2\zeta \quad (C-3)$$

Equating A_c to A_L gives $\zeta = T/2$. A plot of both functions for comparison is shown in figure C-1 .

RELATIVE MAGNITUDE OF FILTER TRANSFER FCN

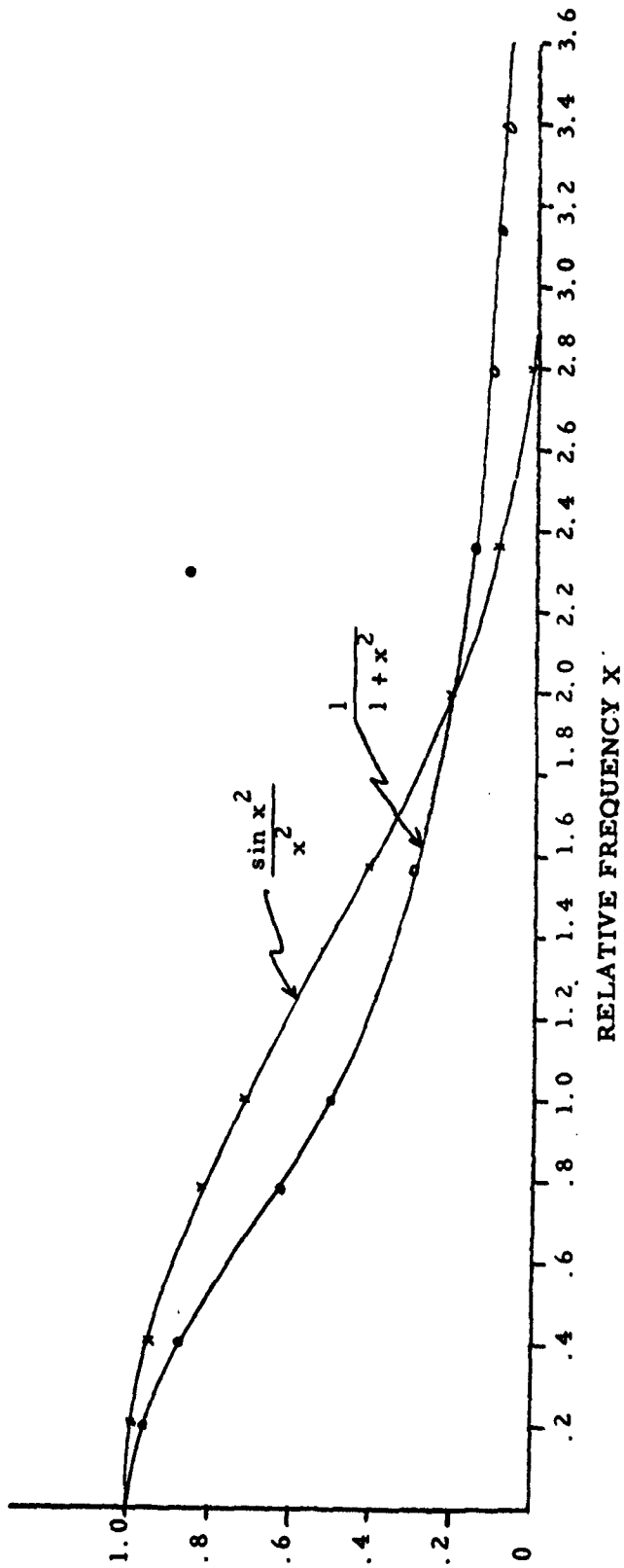


FIG. C-1 RELATIVE MAGNITUDE OF FILTER TRANSFER FUNCTION AS A FUNCTION OF THE RELATIVE FREQUENCY X.

REFERENCES

1. Millican, G. and Jelsma, L., "Radar Electronic Circuitry Utilizing Tunnel Diodes", Final Report, Texas Inst. Inc., Contract AF 30(602)-2314, 10 October 1961.
2. Dickens, L. "The Tunnel Diode: A New Microwave Device", Final Report, Johns Hopkins Univ., Contract AF 33(616)-6753, May 1962.
3. Dickens, L. E., "Progress With Tunnel Diodes", Microwave Journal, V7, pp 70-75, July 1962.
4. Ashby, A, et al, "Evaluation and Improvement of Radar Beacon Systems", Final Report, ARF Project E136, Contract DA 36039 SC85318, 30 June 1961.
5. Smilen, L., "A Theory for Broadband Tunnel Diode Amplifiers", Report No. PIBMRI-998-62, Polytechnic Institute of Brooklyn, Contract AF 30(602)-2213, 20 April 1962.
6. Matthaei, G., et al, "Design Criteria for Microwave Filters and Coupling Structures," Final Report, Stanford Res. Inst., Contract DA 36039 SC74862, Chapter 30, January 1961.
7. Matthaei, G., "A Study of the Amplifiers and Up-Convertors", IRE Trans. MTT, V(MTT9), pp 23-28, January 1961.
8. Fox, Jerome, Editor, Active Networks and Feedback Systems, V(X), MRI Symposium Proc., Polytechnic Press, Brooklyn, N. Y. 1961.
9. Weinberg, N., "Synthesis of Negative Resistance Amplifiers", NEC Proc., Vd.17 pp462-476, October 1961.
10. Green, E., "Synthesis of Ladder Networks to Give Butterworth or Chebyshev Response in the Pass Band", Proc. IRE (London Part IV, Monograph No. 88 (1954).
11. Matthaei, G., et al, "Microwave Filters and Coupling Structures", Third Quarterly, Contract DA36039 SC87398, Stanford Res. Inst., October 1961.
12. Scanlan, J. O., "Properties of the Tunnel Diode", Electronic Technology, pp 269-276, July, 1962.
13. Cohn, S. B., "Properties of Ridge Wave Guide", Proc. IRE, Vol 35, pp 783-788, August 1947.
14. Very High Frequency Techniques, McGraw-Hill Co., New York, 1947, Vol. II, chp. 27.

REFERENCES Con't

15. "Coherent Pulse Doppler Study Program", Final Report, 1- July 1961 to 30 June 1962, Contract No. DA 36-039 SC-87310, AD-282919. Radio Corp. of America, Missile and Surface Radar Div.
16. Bendat, Julius S., Principles and Applications of Random Noise Theory, J. Wiley and Sons, Inc., New York 1958 pp 76.
17. Edson, W. A., "Noise in Oscillators", Proc. IRE Vol. 48, August, 1960 pp 1454-1466.
18. James, H. M., Nichols, N. B., Phillips, R. S. Theory of Servomechanisms, Radiation Laboratory Series, Vol. 25, McGraw-Hill Book Co., Inc., New York 1947.

AD _____	Dir. S/A Accession No. _____
Armer Research Foundation, Chicago, Illinois EVALUATION AND IMPROVEMENT OF RADAR MEASON SYSTEMS R. D. Smalley, S. Kasal, P. P. Toulson Second Quarterly Report 1 September 1963 - 30 November 1963 AF 24 - Res. - 5778 Contract No. DA 36-337-SC-96493	
Declassified 1. Radar becomes 2. Smalley, R. D. 3. Kasal, S. 4. P. P. Toulson 5. U.S.A. Electronics Research and Develop- ment Laboratory Contract No. DA 36-337 SC-96493	
Unclassified Report The results of a partial literature survey on tunnel diode amplifiers are presented. The gap existing between the analytical work and practical design is discussed. Limitations of presently available synthesis techniques are pointed out along with the practical problems which these limitations impose. Results on an experimental C-band amplifier are presented. Sensitivity data on a commercial available backward diode is also presented. The noise power spectrum of a proposed high power harmonic generation system is discussed. Preliminary analysis of a vectorable tunable tunnel diode oscillator is presented. Results of additional theoretical work on the coherent Doppler radar are briefly discussed.	

AD _____	Dir. S/A Accession No. _____
Armer Research Foundation, Chicago, Illinois EVALUATION AND IMPROVEMENT OF RADAR MEASON SYSTEMS R. D. Smalley, S. Kasal, P. P. Toulson Second Quarterly Report 1 September 1963 - 30 November 1963 AF 24 - Res. - 5778 Contract No. DA 36-337-SC-96493	
Declassified 1. Radar becomes 2. Smalley, R. D. 3. Kasal, S. 4. P. P. Toulson 5. U.S.A. Electronics Research and Develop- ment Laboratory Contract No. DA 36-337 SC-96493	
Unclassified Report The results of a partial literature survey on tunnel diode amplifiers are presented. The gap existing between the analytical work and practical design is discussed. Limitations of presently available synthesis techniques are pointed out along with the practical problems which these limitations impose. Results on an experimental C-band amplifier are presented. Sensitivity data on a commercial available backward diode is also presented. The noise power spectrum of a proposed high power harmonic generation system is discussed. Preliminary analysis of a vectorable tunable tunnel diode oscillator is presented. Results of additional theoretical work on the coherent Doppler radar are briefly discussed.	

AD _____	Dir. S/A Accession No. _____
Armer Research Foundation, Chicago, Illinois EVALUATION AND IMPROVEMENT OF RADAR MEASON SYSTEMS R. D. Smalley, S. Kasal, P. P. Toulson Second Quarterly Report 1 September 1963 - 30 November 1963 AF 24 - Res. - 5778 Contract No. DA 36-337-SC-96493	
Declassified 1. Radar becomes 2. Smalley, R. D. 3. Kasal, S. 4. P. P. Toulson 5. U.S.A. Electronics Research and Develop- ment Laboratory Contract No. DA 36-337 SC-96493	
Unclassified Report The results of a partial literature survey on tunnel diode amplifiers are presented. The gap existing between the analytical work and practical design is discussed. Limitations of presently available synthesis techniques are pointed out along with the practical problems which these limitations impose. Results on an experimental C-band amplifier are presented. Sensitivity data on a commercial available backward diode is also presented. The noise power spectrum of a proposed high power harmonic generation system is discussed. Preliminary analysis of a vectorable tunable tunnel diode oscillator is presented. Results of additional theoretical work on the coherent Doppler radar are briefly discussed.	

AD _____	Dir. S/A Accession No. _____
Armer Research Foundation, Chicago, Illinois EVALUATION AND IMPROVEMENT OF RADAR MEASON SYSTEMS R. D. Smalley, S. Kasal, P. P. Toulson Second Quarterly Report 1 September 1963 - 30 November 1963 AF 24 - Res. - 5778 Contract No. DA 36-337-SC-96493	
Declassified 1. Radar becomes 2. Smalley, R. D. 3. Kasal, S. 4. P. P. Toulson 5. U.S.A. Electronics Research and Develop- ment Laboratory Contract No. DA 36-337 SC-96493	
Unclassified Report The results of a partial literature survey on tunnel diode amplifiers are presented. The gap existing between the analytical work and practical design is discussed. Limitations of presently available synthesis techniques are pointed out along with the practical problems which these limitations impose. Results on an experimental C-band amplifier are presented. Sensitivity data on a commercial available backward diode is also presented. The noise power spectrum of a proposed high power harmonic generation system is discussed. Preliminary analysis of a vectorable tunable tunnel diode oscillator is presented. Results of additional theoretical work on the coherent Doppler radar are briefly discussed.	